RESPONSES OF WELL WATER LEVELS ON NORTHERN GUAM TO VARIATIONS OF RAINFALL AND SEA LEVEL

By

Mark A. Lander

John W. Jenson

Colette Beausoliel

WERI

WATER AND ENVIRONMENTAL RESEARCH INSTITUTE
OF THE WESTERN PACIFIC
UNIVERSITY OF GUAM

Technical Report No. 94

MAY 30 2001

Produced with Scantopdf

www.scantopdf.co.uk

www.scantopdf.co.uk

RESPONSES OF WELL WATER LEVELS ON NORTHERN GUAM TO VARIATIONS OF RAINFALL AND SEA LEVEL

By

Mark A. Lander

John Jenson

Colette Beausoliel

Water and Environmental Research Institute
of the Western Pacific
University of Guam
UOG Station
Mangilao, Guam 96923

Produced with ScanTOPDF

www.scantopdf.co.uk

www.scantopdf.co.uk

Abstract

The Northern Guam Lens Aquifer is comprised of Plio-Pleistocene limestone units deposited atop a volcanic basement. Typical heads range from about 3 to 5 feet above sea level, with the maximum thickness of the lens ranging up to about 150 feet. Continuously draining into the ocean, the water in the lens is replenished by rain, which, averages about 100 inches per year, but is highly variable on both long and short time and space scales. Guam draws some 80% of its drinking water from the freshwater lens in the aquifer, using some 45 million gallons per day, a bit more than half of the most recent estimate of 70-80 million gallons per day of sustainable yield. In order to identify appropriate techniques and management practices to sustain aquifer development while protecting water quality, groundwater scientists and engineers need a better understanding of aquifer dynamics. In particular, it will be necessary to better understand the factors that control the rates and amounts of water taken into storage, the residence time of water in the aquifer, and the quantities that can therefore be extracted in given times and places without degrading the quality of the water. The responses of well levels to rainfall events provide important clues regarding the rate at which water descends through the vadose zone, the amount of time that it is retained in phreatic storage, and therefore the amount that may ultimately be available for exploitation by various techniques.

Variations in rainfall and sea level are the most direct and important causes of variations in well levels. Observations from 3 wells in the Agana Argillaceous Member of the NGLA indicate that the combined variations in sea level and rainfall in real time or near-real time account for up to 66% of the variance of water levels in the wells—the sea level accounting for the larger share of this variance near the coast, and the rain accounting for the larger share of the variance at well locations further inland. Multi-year variations of rainfall appear in the well levels at time lags up to nearly two years. Heavy 24-hour rainfalls of up to 3 inches may cause no immediate response of well levels if they occur at the end of prolonged dryness. Similar rain events cause immediate and large increases of well level if they occur during prolonged wet periods. Rapid increases in well levels in response to heavy short-term rain events decay to background levels within a period of about 10 days. The observed response of the wells to variations in the rainfall and sea level suggest a complicated mix of diffuse and open pathways through a heterogeneous limestone medium. Future reports from this project will evaluate the responses of well in the non-argillaceous limestone units of the NGLA and address the degree to which the different lithologies and aquifer properties between the units may drive different aquifer responses to rainfall.

Produced with ScanToPDF

www.scantopdf.co.uk

www.scantopdf.co.uk

Table of Contents

Produced with Scan TOPDF

www.scantopdf.co.uk

www.scantopdf.co.uk

List of Figures

Figure **Page**

Produced with Scantopdf
www.scantopdf.co.uk
www.scantopdf.co.uk

Figure **Page**

List of Tables

Table **Page**

Produced with Scantopdf
www.scantopdf.co.uk
www.scantopdf.co.uk

Introduction

The island of Guam is blessed with an enormous amount of fresh water stored in the thick limestone mantle that covers almost all of the northern half of the island and the eastern fringe of the southern half of the island. The Northern Guam Lens Aquifer (NGLA) provides 80% of Guam's potable water production of more than 40 million gallons per day (mgd) for its 150,000 permanent residents and 1,000,000 tourists who visit the island annually. As limits to production are approached, understanding aquifer characteristics is imperative if the aquifer is to be managed properly to meet future demand and to preserve water quality.

The NGLA is composed primarily of two permeable limestone formations, the Pliocene-Pleistocene Mariana Limestone, and the Miocene-Pliocene Barrigada Limestone (Tracey, et al. 1964). The Mariana limestone was deposited as a shallow-water fringing and barrier reef, and is thickest along the rim of the uplifted northern plateau. The older Barrigada limestone is a deeper-water limestone of bank and off-reef detrital deposits. The Barrigada limestone dominates the interior of the plateau, and accounts for the greatest volume of the aquifer, especially in the island's interior. The basement beneath the limestone is a late Eocene-Oligocene submarine volcaniclasitc deposit with a permeability many orders of magnitude lower than the overlying limestone.

The sustainable yield of the aquifer—defined as the rate of pumpage that can be sustained over the long run without affecting the quality of the water -- has been estimated in previous studies to be from about 60 mgd (CDM, 1982) to upward of 80 mgd (Mink, 1991). Sustainable yield is a global concept, however. Although it provides a useful aggregate benchmark for water resource planning, it provides no guidance for the determining the appropriate pumping rate for a particular well in a particular location. To support such decisions, water resource managers need a sufficiently precise understanding of local hydrogeologic characteristics for each well field to enable reliable prediction on well response to pumping and changes in recharge. As the aquifer approaches the total sustainable yield, it will be more and more important for developers to base decisions regarding the installation or design of a given well on a case-by-case analysis of local properties of the well field and the potential effects that a new well might have on neighboring wells.

Certain hydrologic and geologic factors must be better understood in order for water resource managers to reliably estimate sustainable production rates for individual wells in selected well fields. These include a better knowledge of the rainfall distribution over the island – the complexities of which are only now being revealed by Guam's NEXARD weather radar, and new dense rain gage networks. Another phenomenon that requires more precise understanding is the nature of the pathways taken by rainfall through the limestone matrix. Mylroie and Vacher (1999) have proposed a dual-porosity aquifer in which dissolution-widened fractures are typically superimposed on a high-porosity matrix. The conductivity associated with each component is high, though variable, and can be orders of magnitude different from the other. Previous conductivity studies on Guam suggest regional conductivities from 1-6 km/day (e.g., from Ayers and Clayshulte's 1984 study of tidal-signal attenuation in inland wells) and local conductivities of 1-100 m/day (from pumping tests). Contractor and Jenson (2000) compared numerical simulations to groundwater-level time series data from observation wells on northern Guam. They concluded that temporary storage of infiltrating water in the vadose zone is significant and that infiltration rates are strongly dependent on the seasonal water content of the vadose zone. Optimizing the vadose parameters in the model did not achieve appreciable error-reduction in simulated water levels, suggesting that temporal and spatial variations in

www.scantopdf.co.uk

vadose zone characteristics are insufficiently known and/or that other processes affecting the temporal and spatial distribution of recharge have yet to be discovered. They noted three plausible sources of error; 1) unknown spatial variability of the hydraulic conductivity in the aquifer, 2) unknown variations in evapotranspiration, and 3) large errors introduced, especially under wet conditions, by the dependency of infiltration and storage on precipitation rates on Guam. Continued modeling studies, along with statistical comparison with the historical record and field hydrographic studies were recommended. This paper is an ongoing attempt at the latter. The preliminary results of a study of the effects of variations in rain and sea level on the water-level time series in three observation wells are presented.

Data

Rainfall

There are dozens of rain gages on Guam with varying periods of record and reliability. Four rain gages with long, complete and reliable records are at the Weather Service Meteorological Observatory (WSMO) in Taguac, Andersen Air Force Base (AAFB), the Naval Air Station (NAS) located on the opposite side of the field of the Guam International Airport, and a USGS gage in Dededo (Fig. 1). The WSMO rain gage was deactivated in 1995. Daily (and in some cases hourly) rainfall is available from these sites. Other reliable short-term rain records exist at dozens of locations around Guam, some for short (several year) periods in the early parts of the 20th century, and others for various short periods throughout the 20th century (with some continuing today). Rain at NAS is measured manually at six-hour intervals from a standard National Weather Service 8-inch rain gage. The daily amount is recorded at local midnight. At WSMO, an electronic recording tipping bucket rain gage was used in the later part of the record. Hourly rainfall values are archived for this site. At Andersen air force base, a standard 8-inch manually-read rain gage is used. Rain amounts are recorded every three hours, and the daily amount is tabulated at local midnight. The USGS rain gage at Dededo is an electronically recording tipping bucket gage, and the rain is archived at intervals as short as 15 minutes.

In this report, the water levels were compared only with the rain recorded at NAS. Further work will incorporate information from other rain gages (some closer to the well sites). Even in this preliminary work using only one rainfall time series (at NAS), the correlations between the water levels and the rainfall are quite high. Monthly rainfall for the period October 1983 through April 1997 was obtained from the NAS archives. Daily rainfall from this site was obtained for certain target rainfall events such as island-wide very heavy rain from typhoons or isolated high-intensity events within or following prolonged droughts.

Tide

There are two official tide gages on Guam. One is located at the western entrance to Sumay Cove Marina in outer Apra Harbor. This gage is owned by the National Oceanic and Atmospheric Administration (NOAA). It normally contains an acoustic gage, a back-up analog bubbler gage with a chart recorder, and a tsunami device. Up until the passage of Typhoon Paka on December 16-17, 1997, tide levels were measured at six- minute intervals, with the data sent via satellite telemetry to the NOAA Data Collection Center in Seattle. Paka put the gage out of service. However, it has recently been rebuilt and put back on line. The other gage is located at the top of the ramp to the commercial boats in the Agaña Boat Basin. This gage is administered by the USGS. Water level is recorded every 15 minutes by a digital recorder. The readings from this USGS Agaña Boat Basin gage are used in this report as the primary sea-level time series for

www.scantopdf.co.uk

comparison to the water levels. Tide data from the Agaña Boat Basin site were obtained for the period October 1983 through December 1996. Monthly average sea level was archived from the record of daily mean sea levels obtained from this site. For certain periods of special interest, the raw daily values of mean sea level from this site were used.

Wells

Three wells are examined in this report: A20 (located in Ordot), A16 (located just south of the international airport), and BPM1 (located near the intersection of routes 10 and 15 in Mangilao). Well A16 and BPM1 are located in the area where Tracey et al. (1964) mapped the surface as the Agana Argillaceous Member of the Mariana Limestone. The A-series wells lie in the Agaña Sub-Basin, and BPM1 in the Mangilao Sub-Basin of the NGLA, respectively, as mapped by CDM (1982). The heads in A16 and BPM1 are typically about a meter (3-4 ft) above mean sea level. These are basal wells, i.e., the fresh water is buoyantly supported by underlying sea water. The relatively high head is consistent with the relative inland location of the wells. Well A20 is a parabasal well, i.e., one in which the fresh water rests directly on the underlying volcanic basement, and is therefore not in direct communication with the sea. Head is typically about 14 m (45 feet) amsl. Not surprisingly, water levels at A16 and BPM1 correlate significantly with sea-level variations, while the water level at A20 is unaffected by variations in sea level. Daily and monthly average water levels are available for all three well sites.

NEXRAD

In the summer of 1993, the Air Force installed a Doppler Weather radar east of Barrigada. This radar was part a nationwide upgrade to the weather radars owned and operated by the National Weather Service and the Department of Defense. The Weather Surveillance Radar (WSR), put on line in 1988, provided for the first time, full Doppler coverage to the entire continental United States. Often referred to as NEXRAD (for NEXt generation weather RADar), the WSR 88D instrument was primarily outfitted to provide improved data on local severe weather (tornadoes, large hail, strong winds in squall lines, etc.). A very useful feature of the NEXRAD is an automated system tool that integrates rainfall at the 6-minute time steps that the radar takes to make its volume scan of its environment. Such integrations provide a complete spatial picture of integrated rainfall at a resolution of about a square mile (Fig. 2a,b). Guam's NEXRAD may provide unprecedented details of the magnitude, and the time and spatial scales of the rainfall over Guam.

Methodology

Removing the tidal signal in the well time-series

The correlation of well water levels with the daily and monthly mean sea level is in general a function of distance from shore. All water level time series of the NGLA exhibit statistically significant cross-correlations with the time series of the daily average tide (expressed in feet above mean sea level). The tidal signal is transferred rapidly into the aquifer, and cross-correlations are highest at zero time lag for all periods investigated (daily to monthly). At some wells, the variations of sea level account for upwards of 50% of the variance of the time series of daily and monthly average water levels.

The linear cross correlation value is used to remove the tidal signal from the well water level time series. The cross correlation coefficients between the sea level and the water level of a

www.scantopdf.co.uk

given well can be used in a linear regression to predict the value of one variable given the value of the other. The best prediction that a linear regression can yield is given by

$$(A_i)^* = (r)\,(s_A/s_B)\,(B_i)' + \bar{A} \qquad (1)$$

where: ( )* indicates the predicted value;
( )′ indicates departure from the mean value;
subscript i indicates the i^{th} value of the time series;
s_A and s_B are the standard deviations of variables A and B respectively;
r is the cross-correlation coefficient between variables A and B; and,
the over-bar indicates the mean value of the indicated time series.

Using Equation (1), the water level may be predicted from the sea-level time series. An adjusted well-level time series that is not correlated with the sea level may be obtained by subtracting the i^{th} term on the right-hand side of equation (1) from the i^{th} raw value of the well-level time series. In this manner, the well-level time series is "de-tided". Note that the well water level time series may be similarly adjusted to "de-rain" the time series, or to remove the component of any variable that has a non-zero cross-correlation with the water level. In this report, the sea-level signal was always removed first in order to evaluate the relationship of the remaining "de-tided" time series to the rainfall. Maximum correlations of water level with rainfall tended to occur at a time lag, whereas maximum correlations of water levels with sea level were always simultaneous at the frequencies examined (daily and monthly).

Using rainfall and tide to predict water levels

The "de-tided" water level time series may be cross-correlated with any other time series (such as time series of rainfall) to form a multiple linear regression equation of the form:

$$(A_i)^* = (r_{A:B})\,(s_A/s_B)\,(B_i)' + (r_{A:C})\,(s_A/s_C)\,(C_i)' + \bar{A} \qquad (2)$$

where: ( )* indicates the predicted value;
( )′ indicates departure from the mean value;
subscript i indicates the i^{th} value of the time series;
s_A, s_B, and s_C, are the standard deviations of variables A, B and C respectively;
$r_{A:B}$ is the cross-correlation coefficient between variables A and B;
$r_{A:C}$ is the cross-correlation coefficient between variable A (signal of B removed) and variable C; and,
the overbar indicates the mean value of the time series.

Such an equation derived to predict the level in well BPM1 from the rain and tide

$$(BPM1_i)^* = 0.5281\,(TIDE_i)' + 0.02227\,(RAIN_i)' + 2.723 \qquad (3)$$

yields a predicted time series for BPM1 that explains 66% of the variance of the raw time series. An investigation of the analysis of the variance explained by the rain and the tide (and the inter-relationships among other variables, such as the wind and the tide) at several well sites occurs in a later section.

Produced with Scantopdf
www.scantopdf.co.uk
www.scantopdf.co.uk

Integrated anomalies

All of the variables examined in this report (rainfall, the Southern Oscillation Index or SOI, sea level, and water levels) were subjected to an analysis wherein the long-term annual or monthly mean of the variable is removed and the anomalies of each variable are added in sequence to create a time series of the running total. These running totals, or "integrated anomalies," sharply highlight long-term deficits or surpluses. The running totals of all the variables show prominent long-term deficits and surpluses that are clearly inter-related.

Guam's Tidal Variations

Basic characteristics of the astronomical tide

Guam experiences a mixed semi-diurnal tide that features a daily maximum high tide, a second slightly lower minimum high tide, a daily maximum low tide, and a second substantially lower minimum low tide. For public purposes, tides on Guam are expressed in feet above mean minimum low tide (mean low low water). In this report, the mean sea level is the average integrated sea level, and water levels are recorded as feet above this mean sea level (amsl). The mean sea level is about 1.5 feet higher than the mean low low water mark. Guam's two daily high tides are roughly equivalent at an average height of about 2.3 feet. The higher of the low tides is only slightly lower than the high tides with a mean height of about 1.5 feet. The low low tide is the most extreme swing of tide level on Guam and is the zero reference for public tide predictions.

The position of the moon relative to the sun (and the positions of both the moon and the sun relative to the earth's equator) produce important variations in the range and symmetry of the daily tides. When the moon is over the equator, the two high tides and the two low tides become more nearly symmetrical. When the moon is farthest north or south of the equator, the asymmetry of the tides is increased: the low low tide becomes markedly lower than the high low tide. This effect is most pronounced during the new and full moons at the time of the solstices when both the moon and the sun are farthest off the equator. At such times, the high high tide rises to its annual peak of +2.7 feet and the low low tide drops to -0.9 feet below the mean low low water mark (Fig. 3a). Despite the marked variation in the character of the tides throughout the year, the mean monthly astronomical sea level varies only slightly (Fig. 3b); it is highest during the solstices, and lowest during the time of the equinoxes.

Observed tidal variations: non-astronomical factors

Whereas the timing and range of Guam's daily high and low tides generally fall in line with astronomical effects, the background sea level on monthly and interannual time scales is not controlled by the sun and moon, but rather, the local and Pacific basin wind flow and seasonal changes in the mixed layer salinity and temperature. The actual mean monthly tide recorded at Agaña Boat Basin (Fig. 4a) exhibits substantial non-astronomical variations. A 13-year average of the mean monthly sea level values shows that the peak monthly mean sea level during the year occurs in July and August, and the lowest monthly mean sea level occurs in December and January (Fig. 4b).

Large observed interannual differences in mean sea level are related in part to El Niño/Southern Oscillation (ENSO). During a typical El Niño, the sea level falls during the autumn of the El Niño year, and bottoms out during the spring of the year following the El Niño

www.scantopdf.co.uk

(especially during major ENSO events like 1982/83 and 1997/98). During periods of prolonged east wind anomalies in the tropical Pacific basin, the sea level tends to be elevated on Guam. A good proxy for the strength of the easterly wind flow across the tropical Pacific is the Southern Oscillation Index (SOI). A measure of the relative sea-level pressure difference between eastern and western portions of the tropical Pacific basin, the SOI is positive when the wind is anomalously easterly and negative when the winds become anomalously westerly. A comparison of the Guam sea level with the SOI (Fig. 5) reveals a strong relationship that is consistent with below normal sea level during times of relaxed tropical Pacific basin easterly wind flow and higher sea level during times of strengthened easterly wind flow.

On a local scale, the wave set-up created by unusually strong and prolonged episodes of monsoonal westerly winds in summer tends to elevate the sea level on the west side of the island. With local exposure to the north at the Agaña Boat Basin tide gage site, high winds from the north or northwest associated with nearby tropical cyclones cause wind and wave set-up at the tide gage site that can elevate the daily mean sea level over one foot above normal. It turns out that a small positive correlation of Guam's daily mean sea level with rainfall is largely a function of an enhanced northerly component of the wind that precedes and often accompanies the large rain events associated with tropical cyclones (Fig. 6). Such complexities of the inter-relationships among the water levels, sea level, rainfall, and other climate variables abound; necessitating extreme scrutiny of every data record and its accompanying metadata.

Guam's fresh water lens is bounded by sea, and is strongly affected by variations of the sea level. The response of the groundwater levels to changes in sea level is rapid. In the wells observed, it appears to be at least as rapid as the variation in the daily mean sea level (the shortest record length examined in this report). From personal observation of water levels in near-shore sink holes and water caves, the water level at many near-shore locations in Guam's aquifer shows a rapid and direct response to the daily high and low tides. Variations in sea level (from daily to monthly to multi-year anomalies) are a major component of the changes in the water levels (see later discussion for more details of the effects of sea level on water levels).

Guam's Rainfall

Total rainfall and aquifer recharge

Inhabitants of Guam recognize two major seasonal divisions of the year based on the local climate—the wet season and the dry season. The dry season generally comprises the first half of the calendar year (January through June), and the wet season typically occurs from July through December. Guam's mean monthly rainfall follows a roughly sinusoidal curve that falls to a minimum of about 3 inches in March and rises to a maximum of 15 inches in August and September. The comfort level of the dry season is accentuated by persistent east-northeast tradewinds averaging 15-20 mph. During the summer, the *mean* wind becomes almost calm -- the result of periods of light winds from the east being interspersed with shorter episodes of brisk monsoonal winds from the southwest.

An average of roughly 100 inches (2540 mm) of rain falls on Guam during the calendar year. Even though the island is quite small (535 km^2) and its mountains are relatively low (401 m or less), the distribution of rainfall on the island is strongly affected by the topography, and the mean annual rainfall totals among recording stations on Guam differ by as much as 30 inches (760 mm). The region in the vicinity of Guam's international airport and the area in the vicinity of Sumay (inner Apra Harbor) receives the lowest annual total of about 85 inches (215 mm)

Produced with Scan to PDF
www.scantopdf.co.uk
www.scantopdf.co.uk

(Guard, 2000). The highest annual total of 115 inches (2920 mm) occurs in the vicinity of the Fena Lake and its watershed, and from there southward along the eastern slopes of the southern mountains.

Other relative minima of annual rainfall occur along the northwest coast and along the southern coast. Another relative maximum of roughly 100 inches (2540 mm) occurs in a NE-SW oriented band that stretches across Guam's northern limestone plateau from the cliff line of Tarague beach on NE Guam to Puntan Dos Amantes (Two-lover's Point) on the west side, just north of Tumon bay. Given Guam's area of 535 km^2, and an average annual rainfall of 100 inches (2040 mm), one can calculate that about 1.1 billion cubic meters (290 billion gallons) of water are deposited on Guam each year. Jocson et al. (1999) showed that about 20% of rainfall arrives in small amounts (< 0.6 cm/day) under dry conditions and is therefore probably lost to evapotranspiration. About another 20% arrives at very high intensities (> 5.0 cm/day) and therefore is probably not captured in long-term phreatic storage. Calculations of recharge based on differences between daily rainfall minus daily pan evaporation suggest that the maximum annual amount of water delivered to the freshwater lens is about 67% of mean annual rainfall (Jocson, 1998). Results of previous work (CDM, 1982) estimated recharge at about 60% of mean annual rainfall, upon which an associated estimated sustainable yield of 3.1-3.5 m^3s^{-1} (70-80 mgd) was based. Three general types of information are essential for refining sustainable yield estimates: (1) how much water is actually captured and stored in the lens in a given sub-basin, (2) how the sub-basin will respond to given total level of extraction over time, and (3) how a given well will respond to a given pumping rate over time. The investigation reported here gives insights into each of these questions. Correlating well responses with seasonal aquifer conditions and rainfall rates provides a starting point for ultimately estimating how much of the annual rainfall drains too rapidly out to the sea to be captured in storage. Such insights also provide a basis for more precisely characterizing the differences in storage and transport characteristics between sub-basins. And the response of observation wells to seasonal aquifer conditions and different rainfall intensities may provide insight to help predict or explain the behavior of nearby production wells.

Rainfall variability

At the Taguac Weather Service Meteorological Observatory (WSMO), the mean annual rainfall during the period 1957-92 was 101.84 inches with a standard deviation of 22.2 inches. The mean dry-season (January through June) rainfall was 31.63 inches with a standard deviation of 16.62 inches; the mean wet-season (July through December) rainfall was 70.21 inches with a standard deviation of 9.79 inches. The wet-season/dry-season split of the annual total is thus about 70% and 30%, respectively. The driest annual total in the time series is the 67.06 inches recorded in 1983. The WSMO was deactivated in 1995, so it was not recording during 1998—which was probably Guam's driest year in the past century. The wettest annual total in the time series is the 165.91 inches recorded during 1976. The wettest dry season (93.89 inches) occurred in 1976, and the driest dry season (9.59 inches) occurred in 1983. The wettest wet season (92.08 inches) occurred in 1962, and the driest wet season (50.50 inches) occurred in 1973. Nearly all extremely dry years on Guam occur during the year following an El Niño event.

The lowest mean (4.06 inches) and median (2.66 inches) monthly rainfall occurs in March. The highest mean monthly rainfall (15.17 inches) occurs in August; however, the highest median monthly rainfall (14.40 inches) occurs in September. Monthly rainfall values below one inch have occurred in February through June. Monthly rainfall values above 20

www.scantopdf.co.uk

inches have occurred in January, May, July, August, September, October, and December. The lowest value of the monthly time series of the rainfall at the Taguac WSMO is the reading of 0.50 inches during April 1965. The highest monthly value is the 40.13 inches recorded during May 1976, of which Typhoon Pamela contributed 27.01 inches—Guam's record 24-hour rainfall.

A study of the distribution of the daily rainfall values within each month shows that nearly half of a given month's total rainfall is typically accrued during the wettest 3 days of the month (Fig. 7). There is quite a bit of scatter about the generic curve shown in Fig. 7; for example, during some months with typhoons, the highest one-day rainfall may comprise 50-75% (or more) of the monthly total, and during other months, the curve is not as skewed. Using the generic curve of Fig. 7, one can say the following of a month with 10 inches of rain:

1) the rainfall exceeded 2 inches in 24 hours on one day,
2) the rainfall equaled or exceeded one inch in 24 hours on three of the days,
3) the rainfall equaled or exceeded 0.50 inches in 24 hours on 7 days,
4) the rainfall was less than 0.10 inches in 24 hours on 13 days.

For a month with only three inches of rain one can say:

1) the rainfall exceeded 0.5 inches in 24 hours on one day,
2) the rainfall equaled or exceeded 0.3 inches in 24 hours on three of the days,
3) the rainfall equaled or exceeded .15 inches in 24 hours on 7 days, and
4) the rainfall was less than 0.10 inch in 24 hours on 20 days.

There is a tendency for the curves to be more highly skewed in the dry season. The daily rainfall distribution given by the generic curve (Fig.7) needs to be altered slightly for such months so that higher daily rainfall amounts are squeezed into fewer days, and lower daily rainfall rates occur more often.

The Taguac rain gage was deactivated in 1995. Other reliable long-term rainfall records exist at Andersen Air Force Base, the Guam International Airport, and at a site in Dededo maintained by the USGS. Daily (and in some cases hourly) rainfall is available from these sites. Other reliable short-term rain records exist at dozens of locations around Guam, some for short (several year) periods in the early parts of the 20th century, and others for various short periods throughout the 20th century (with some continuing today). Water levels are strongly linked to short and long-term variations in rainfall, which along with variations in sea level, are the primary forcing mechanisms for water level changes. Subsequent sections of this report examine these relationships in more detail.

Rain-producing weather systems

Guam is located in a region of the world characterized by large-scale seasonal weather changes associated with the monsoons of the Eastern Hemisphere. For most of the year, the winds on Guam are from the east, but during the summer and early autumn, the winds can become west to southwest for periods lasting up to one month. Generally, the swing of wind to the SW is episodic and occurs in 3 to 10 day periods during which the winds may approach gale force. The number, strength and duration of episodes of SW winds on Guam is highly variable from year to year. The wind may become southwesterly on Guam at any time of the year when a tropical cyclone passes to the north of the island.

Produced with Scantopdf
www.scantopdf.co.uk
www.scantopdf.co.uk

Much of Guam's wet-season rainfall is derived from cloud clusters and tropical cyclones that form in or near the monsoon trough. The general properties of the monsoon trough of the western North Pacific (WNP) follow:

(1) It is elongated east-west,
(2) It is a nearly linear shear zone between easterly and southwesterly wind currents,
(3) It possesses a nearly linear east-west oriented cloud band with most of the cloudiness and deep convective elements located to the south of the trough axis, and
(4) It is the genesis site of most of the tropical cyclones of the WNP.

The monsoon trough generally becomes firmly established in the WNP basin in July, and it is usually during July that the trough makes its first migration to the north of Guam bringing the first episode of SW monsoon winds. Throughout the summer, the monsoon trough undergoes substantial migrations and major changes to its shape and orientation. Tropical cyclones further complicate the flow pattern as their frequency of formation increases. A very vigorous monsoon trough established to the north of Guam can bring strong SW winds, cloudy wet weather, and rough seas on the western shores. Intense squalls with gales and white-out conditions in heavy rain often accompany the southwest monsoon flow (these can easily be mistaken by residents for tropical cyclones). A strong monsoon trough and tropical cyclone formation go hand in hand.

By November, the axis of the monsoon trough moves southward from its mean summer location and extends further to the east. Westerly winds blow at low latitudes of the WNP, and a second monsoon trough axis develops in the southern Hemisphere (at this time of year, these monsoon troughs are sometimes called, "near equatorial troughs"). At the arrival of the boreal winter, the monsoon trough of the Northern Hemisphere disappears as northerly winds cross the equator and then turn to become the northwesterly flow of the Australian Northwest Monsoon. By early January, the monsoon trough axis of the Southern Hemisphere becomes firmly anchored across northern Australia eastward into the Solomon Islands. In addition, tradewind flow becomes firmly established over Guam, and the character of the cloudiness and rainfall on Guam (apart from relatively rare off-season tropical cyclones) becomes that of a tradewind regime.

Wet season weather systems

During the wet season, the atmosphere over Guam becomes deeply moist and less resistant to vertical ascent of low-level air into towering convective clouds. Large billowing thunderheads (deep convective clouds) can grow vertically to great heights (55,000 ft or more) and produce very heavy deluges of large-drop rainfall. The origin of most of the wet season rainfall can be attributed to deep convective clouds in various stages of organization and/or life cycle. Deep convection can be in the form of an isolated towering cloud column (which may produce a heavy downpour over only a very small area (e.g., a square kilometer), or individual large convective clouds may coalesce into larger clusters known as Mesoscale Convective Systems (MCSs) (Maddox 1980). An MCS may cover 10,000 to 50,000 square kilometers and produce steady moderate to heavy rainfall over a similar large area. Prolonged island-wide downpours are often attributable to the formation (or passage) over Guam of an MCS. Two other important organized forms of convective clouds are the tropical cyclone (with its core convection and peripheral rainbands) and monsoon squall lines.

www.scantopdf.co.uk

In summary, wet-season precipitation is predominantly of convective origin. Much of the wet-season precipitation falls as heavy downpours from individual active convective clouds although some wet-season rain derives from stratiform (i.e., "flat," or "layered") clouds which are the decaying remnants of a prior MCS. Heavy downpours from isolated convective clouds may cover only small portions of the island at a given time (see Fig. 2a). Larger-scale heavy rain events may result from the formation or passage over Guam of an MCS. Rainfall from the passage of a tropical cyclone over the island produces the largest 24-hour values, and the most widely distributed heavy rain possible. In order of the spatial scale (small to large) of the heavy precipitation, the causes of wet-season heavy rain events (e.g., total daily precipitation on the order of 100 mm or greater) are:

1) Individual isolated thunderstorm cells,
2) Formation, or passage, of an MCS over the island,
3) Squall lines in strong southwesterly monsoon flow,
4) Convective cloud bands in the peripheral flow of a tropical cyclone, and
5) Direct passage over the island of the central MCS of a tropical cyclone (or in the case of a typhoon, the eyewall).

Extreme gradients of rainfall are seen in the summer, especially in conditions of isolated thunderstorms. Twenty-four hour storm-total rainfall gradients on the order of 100 mm per kilometer are common (Fig. 2a). Weather systems with larger spatial scales may produce substantial rainfall over the whole island with lesser, but still quite large, spatial gradients. Guam's NEXRAD Doppler weather radar has proven to be a valuable tool to determine the amounts and gradients of rainfall over the entire island.

Dry season weather systems

The dry season on Guam is dominated by tradewinds. In a tradewind regime the air is subsiding, clouds lack vertical development, and rainfall comes in the form of sporadic tradewind showers. Although the rainfall in tradewind showers may be locally heavy, its normal character is brief spates of light to moderate rainfall. Daily rainfall totals rarely exceed .25 inches. A good one-third of all dry season days feature either no rain or just a trace. The tradewind flow is usually peppered with a random distribution of clusters of tradewind showers. Thus, even during the dry season, a few light showers are experienced on most days, but the accumulated amounts are usually very small. On rare occasions, clusters of showers in the tradewind flow may produce daily rainfall totals of up to one inch, often in an east-west stripe across a portion of the island (e.g., Fig. 2b). Another rarely occurring cause of substantial rainfall in the dry season is the northward spread of clusters of thunderstorms (that remain common south of 10°N during Guam's dry season) to Guam's latitude that bring a heavy rainfall event of convective origin.

Two types of large-scale weather systems can bring substantial (an inch or more in a day) rainfall to Guam during the dry season: an off-season tropical cyclone, and a "shear line." During the period 1960-1990, the Joint Typhoon Warning Center (JTWC) (on Guam until its move to Hawaii in 1999) recorded an average of 5.5 tropical cyclones in the WNP basin during the dry season (JTWC 1990) with a monthly distribution as follows:

January – 0.6	March – 0.5	May – 1.3
February – 0.2	April – 0.7	June – 2.2

www.scantopdf.co.uk

During the period 1945-1990, twenty-six tropical cyclones passed within 180 n mi of Guam during the dry season (an average of about one such tropical cyclone every other dry season). Tropical cyclones have been responsible for daily rain totals of six inches or more in each of the dry season months. Ironically, the wettest month recorded on Guam was a dry season month (May 1976) that featured 27.01 inches in one day from the passage of Typhoon Pamela over the island.

The other important rain-producing large-scale weather system of the dry season is the "shear line." A "shear line" accompanies (or can be said to be) the band of clouds and showers which are the extension into the tropics of the cloud band associated with the cold fronts of the large extratropical storm systems which traverse the mid-latitudes of the North Pacific. Rather than the abrupt and relatively large directional shift of the wind experienced with the passage of a cold front in the mid-latitudes, a "shear line" passage in the tropics or subtropics often brings a dramatic strengthening—but little change in direction—of the prevailing tradewind flow. The character of the rain on Guam produced by a shear line is typically a prolonged period of episodic light to moderate showers and periods of misty drizzle. At times there are embedded heavier showers, and occasionally there is even an outbreak of deeper convective rain clouds along the leading edge of a shear line. Rainfall totals of .50 inch to over one inch are common during the one-to-two day passage of a strong shear line cloud band over Guam.

Water Levels in Observation Wells

Hydrogeological conditions

BPM1. The period of record is October 1981 through December 1996. Well BPM1 is located about a mile inland from the cliff edge facing southeastward to the Pacific Ocean. The average head in this well is 2.71 feet above mean sea level (amsl), ranging from a low of 2.21 feet amsl in May 1991 and March 1995 to a high of 3.31 feet amsl in September 1996 (with a close 2nd of 3.24 feet in September 1992 following a very wet August). The average monthly head peaks in September at 2.91 feet amsl, and bottoms out at 2.59 feet amsl in January (Fig. 8).

A-16. The period of record is October 1981 through September 1995. Well A16 is located just south of Guam's International Airport. This location is in the middle of the island, approximately 3 miles inland from the sea to both the east and west. The average head is 3.60 feet above mean sea level (amsl), ranging from a low of 3.02 feet amsl in May 1991 (with a close 2nd of 3.09 feet amsl in March 1995) to a high of 4.17 feet amsl in September 1992 (following a very wet August). The average monthly head peaks in September at 3.83 feet amsl, and bottoms out at 3.46 feet amsl in May. The water level remains nearly constant at about 3.5 feet amsl from January through June. (Fig. 8).

A-20. The period of record is January 1978 through February 1992. Well A-20 is located in Ordot at about the exact geometric center of the island. It is about a 3 miles inland from the ocean. Because A-20 terminates in the parabasal zone of the aquifer (where the base of the freshwater lens is perched on the relatively impermeable volcanic basement rock that rises well above sea level in this location), the average head is 41.3 feet above mean sea level (amsl), ranging from a low of 30.9 feet amsl in October 1978 to a high of 52.6 feet amsl in January 1986. The mean monthly wellhead peaks in February at 47.3 feet amsl, and bottoms out at 35.9 feet amsl in September (Fig. 8).

www.scantopdf.co.uk

As noted earlier in this report, all three of the wells lie in the area in which Tracey et al. (1964) assigned the surface unit to the Agana Argillaceous Member of Mariana Limestone. Tracey et al. mapped some inliers of Alifan Limestone within this unit and speculated that the Alifan Limestone may extensively underlie the Argillaceous Member. The Alifan Limestone is a much older (Miocene-Pliocene) limestone that much more thoroughly indurated from recrystallization and consequently has significantly lower small-scale porosity. (It has long been the rock of choice on the island for aggregate for concrete and road mettle.) Regional hydraulic conductivities tend to be about an order of magnitude smaller in wells installed on the Agana Argillaceous Member than elsewhere in the aquifer, where the bedrock is dominated by the Plio-Pleistocene Barrigada Limestone (a shallow bank to lagoonal detrital deposit), which grades upward and outward into the Pleistocene Mariana Limestone (a lagoonal and back-reef to reef deposit). Local hydraulic conductivities everywhere tend to be about an order of magnitude less than regional conductivities (Mink and Vacher, 1997).

An important characteristic of the Agana Argillaceous Member is that, in contrast to the other limestone units of the aquifer, the terrain formed on it exhibits classic karst features such as disappearing streams, blind valleys, and collapse sinkholes. Why this is so is not well understood yet, but the development of such features is certain to be related to the generally lower regional-scale hydraulic conductivity, presumably because associated lower rates of infiltration support the development of a surface drainage network that distributes surface runoff during higher-than-average precipitation events. On the other hand, the development of a classic karst terrain in this area suggests that it contains enhanced secondary porosity, presumably dissolutionally enlarged fractures and conduits that carry water between the associated surface features. The hydrogeologic characteristics of the area in which the three wells examined in this study are located are, therefore, significantly different from those of the rest of the aquifer. It is therefore important to keep in mind that until a similar analysis is conducted on the wells in the rest of the aquifer, the observations and conclusions drawn from the three wells examined in this study may not necessarily be representative of the aquifer as a whole. This does not diminish the importance of the study reported here, however, since the area covered by the Agana Argillaceous Member constitutes a significant portion of the aquifer, and has properties that should provide insight into the behavior of the rest of the aquifer.

Effects of rain and tide

A five-month moving average of Guam's rainfall for the period 1960-99 (Fig. 9) shows high year-to-year variability. Much of this year-to-year variability is related to the ENSO, with some of the driest years occurring in the year following EL Niño (e.g., 1966, 1973, 1983, 1988, and 1998). Multi-year (decade-scale) variations in Guam's rainfall are suggested by Fig. 10. The early 1960s appear to have been wet, followed by a prolonged long-term deficit of rainfall between the breakpoint years of 1965-1983. From 1984 to the breakpoint year of 1997, the integrated rainfall shown in Fig. 10 rises. From 1998 onward, a new period of long-term precipitation deficit begins. Superimposed on the long-term rise and fall of the integrated rainfall are sharp peaks and troughs that are primarily associated with ENSO: the period from the end of the El Niño year through the year following El Niño tends to be very dry.

The annual cycle of rain is a dominant signal in the well-level time series. Linear regression analysis reveals that at BPM1 and A16 the best correlation of rain with water level was obtained by combining the rain of the current month with that of the prior month. Well A20, on the other hand, exhibits a nearly six-month time-lag response to the annual cycle of rain. (See

www.scantopdf.co.uk

the later discussion of the *prediction skill of linear regression* for a more complete discussion of the water level variations associated with rainfall.)

As with the rainfall, long-term integrations of well-level anomalies also show multi-year integrated deficits and surpluses (Fig. 11). There is some suggestion that the multi-year deficits and surpluses of the water levels lag the rainfall deficits and surpluses by up to 2 years (Fig. 12). These long-lag responses are consistent with the theoretical predictions of Contractor and Jenson (2000) who used a one-dimensional Darcian vadose model to examine optimized vadose transport rates for the aquifer. The authors of this technical report plan to direct future work toward empirical analysis of the long-term groundwater level trends and the role of vadose transport in modulating the seasonal and trans-seasonal signals in rainfall distribution.

At the temporal scales investigated (daily-averaged to monthly-averaged), the response of the water levels to the sea level is simultaneous. In A20, the freshwater lens is not in contact with the sea, so water levels show no correlation with sea level variations. Not surprisingly, the relative contribution of sea level variations to the water level appears to diminish inland where variations in rainfall dominate. For wells in which the freshwater lens is underlain by marine water, up to 66% of the variance in the water-level time series can be accounted for by variations in rainfall and sea level (see the later discussion of the *prediction skill of linear regression*).

Selected heavy rain events

Five high intensity 24-hour rainfall events were chosen to examine the response of water level to high rain events: Tropical Storm Carmen, October 1986 (Fig. 13a); Typhoon Roy, January 1988 (Fig. 13b); Typhoon Russ, December 1990 (Fig. 14a), Typhoon Omar, August-September 1992 (Fig. 14b); and Tropical Storm Verne and Typhoon Wilda, October 1994 (see earlier Fig. 6). In each of these events island-wide maximum 24-hour rainfalls exceeded 3 inches.

An evaluation of the well response due to the first four typhoon events (Fig. 15) reveals substantial variations. In general, after an extreme typhoon-related rainfall event, the water level rises rapidly to a peak within one or two days, and then the water level drops off in a roughly logarithmic decay with an e-folding time of about 4 days. The level falls back to near the pre-event value in about 10 days. In most cases, the magnitude of the water level rise is greater than the rainfall amount. For example, the 4.2 inches of rain during October 11-12, 1994 led to a 7.2 inch rise in the level of BPM1. The extreme case is the rise of almost three feet in well A16 after 11 inches of rain on August 28 in Typhoon Omar. An opposite case is the rise of only 8 inches in well A16 after almost 11 inches from Typhoon Russ.

The variables controlling the magnitudes and variation between these responses are undoubtedly complex. Some of the variation may possibly be explained by the distribution of rain during the respective typhoon event. During Typhoon Omar, most of the rainfall occurred on the northern half of the island, with a maximum on the very northern-most one-third of the island. Thus the 11 inches of rain estimated for Omar at NAS and the WSMO was likely a lower value than at locations further north. The resulting water level rise at A16 (mid-Guam) likely reflected the higher rains to the north. An odd case is seen with the well response to the rains of Typhoon Roy. Here there is three-day delay in the upward spike of the water level. Typhoon Roy passed to the north of Guam, and rains of 6 inches or more were experienced only in the northern one-third of Guam. The rain at NAS was approximately 3 inches. It is hypothesized that the Roy case shows the delayed passage of a water pulse at the well site generated by heavy rain in the northern reaches of the NGLA. The opposite behavior is seen with Russ. The rise in

www.scantopdf.co.uk

the well level is lower than the rainfall amount, and occurs one day after the event. Russ passed to the south of the island, and the heaviest rains were over the southern half of Guam. Rainfall amounts diminished northward, and hence a quick rise to peak at the well, and a lower magnitude of well-head increase than the rainfall at NAS.

There are likely other important factors in addition to rainfall distribution, however, that control the magnitude and time of well-level responses to rainfall. First, the relationship between rainfall intensity and surface infiltration rate at any given location may exert an important influence on the degree to which stormwater is redistributed at the surface and shunted into sinkholes or other features that may be connected to vadose by-pass routes, which could shunt stormwater more or less directly to the freshwater lens. Within the aquifer, the distribution of effective porosity, including the distribution, capacity, and connectivity of open vadose pathways, may be important. Finally, the pathway taken by vadose water (i.e., diffuse flow through the matrix versus concentrated flow down vadose bypass routes) appears to be strongly sensitive to the pre-existing degree of saturation of the vadose matrix, which controls the rate and extent to which new vadose water will be captured in storage or shunted down open pathways (Jocson et al., 1999; Contractor and Jenson, 2000). As previously noted by Jocson et al. (1999) after periods of prolonged dryness, observation wells show little or no response to the first heavy rain event to break the drought (Fig. 16).

Prediction skill of linear regression

BPM1. BPM1 was the first well for which a multiple linear regression was used to predict the water level using the TIDE and RAIN time-series. The analysis was based on monthly mean well water levels, monthly mean sea level and total monthly rainfall measured at NAS. The first step was to determine the contribution of sea-level variations to variations in the water level. The correlation between the monthly mean BPM1 water level and the monthly mean sea level, $r = cor$(BPM1:TIDE), was 0.72. The correlation between the monthly mean BPM1 water level and the monthly rainfall, $r = cor$(BPM1:RAIN), was 0.56. The highest correlation value for (BPM1: TIDE) was obtained at a zero time lag, however, the highest correlation value for (BPM1: RAIN) was obtained by incorporating information from the month at zero time lag with the prior month (i.e., the best correlation between BPM1 and RAIN was with the new variable, $[month_{(0)} + month_{(-1)}]/2$. A prediction equation of the form of equation (2) yielding predicted values for the water level in BPM1 given information about the TIDE and RAIN is given by

$$Predicted\ BPM1_i = 0.5281\ (TIDE_i)' + 0.02227\ (RAIN_i)' + 2.723$$

The correlation coefficient between the predicted BPM1 and the raw values of BPM1 (Fig. 17) is .81. Thus, 66% of the variance of the BPM1 time series is explained by the TIDE and RAIN.

A16. The next well for which multiple linear regression was used to predict the water level using the TIDE and RAIN time series was A16. Monthly mean water levels, monthly mean sea level, and monthly rainfall totals at NAS were used. The first step was to determine the contribution of tidal variations to variations in the water level. The correlation between the monthly mean A16 levels and the monthly mean tide, $r = cor$(A16:TIDE), was 0.52. The correlation between the monthly mean A16 levels and the monthly rainfall, $r = cor$(A16:RAIN), was 0.59. As with BPM1, the highest correlation value for (A16:TIDE) was obtained at a zero time lag, and the highest correlation value for (A16:RAIN) was obtained by incorporating

www.scantopdf.co.uk

information from the month at zero time lag with the prior month (i.e., the best correlation between A16 and RAIN was with the new rain variable, $[month_{(0)} + month_{(-1)}]/2$. A prediction equation of the form of equation (2) yielding predicted values for the water level in A16 given information about the TIDE and RAIN is given by

$$Predicted\ A16_i = 0.3565\ (TIDE_i)' + 0.02473\ (RAIN_i)' + 3.593.$$

The correlation coefficient between the predicted A16 and the raw values of A16 (Fig. 18) is .74. Thus, 54% of the variance of the A16 time series is explained by the TIDE and RAIN.

A20. Well A20 behaved very differently from wells BPM1 and A16. This is attributable to the parabasal character of the well: the water level in A20 is approximately 45 feet (much higher than the approximately 3 feet well heads of the other two wells), and that the water level in A20 was not affected by the tide. The correlation between the monthly mean water levels and the monthly rainfall, $r = cor$(A16:RAIN), in A20 was 0.73. This was the highest correlation of any of the wells with RAIN. There is more to the story, however, in that this high correlation of A20 with RAIN was obtained at a 5 to 6 month time lag. Thus, a new RAIN variable, $[month_{(-5)} + month_{(-6)}]/2$, gave the highest correlation value of 0.73 for (A20:RAIN) (Fig. 19). Table 1 summarizes the results of the linear regression analyses of monthly mean water levels, monthly mean sea level, and monthly rainfall follows:

Well	Strongest effect on well water level exerted by:	Time Variable for RAIN	Percent variance explained by TIDE	Percent variance explained by RAIN	Percent variance explained by prediction equation
BPM-1	Tide	$[month_{(0)} + month_{(-1)}]/2$ (no lag for TIDE)	51% $r = .72$	31% $r = .56$	66% $r = .81$
A-16	Rain	$[month_{(0)} + month_{(-1)}]/2$ (no lag for TIDE)	27% $r = .52$	34% $r = .59$	54% $r = .74$
A-20	No tidal influence	$[month_{(-5)} + month_{(-6)}]/2$	0%	53% $r = .73$	

Table 1. Summary of results from linear regression analyses of the monthly mean well water levels, monthly mean sea level, and monthly total rainfall.

Produced with Scantopdf
www.scantopdf.co.uk

Concluding remarks

Variations in rainfall and sea level cause variations in well water levels. The combined variations in sea level and rainfall in real time or near-real time account for up to 66% of the variance of water levels in the wells, with sea level accounting for the larger share of this variance near the coast, and the rain accounting for the larger share of the variance at well locations further inland. There is evidence that multi-year variations of rainfall appear in the water levels at time lags up to nearly two years. Heavy 24-hour rainfalls of up to 3 inches may cause no immediate response of water levels if they occur at the end of prolonged dryness. Similar rain events cause immediate and large increases of water level if they occur during prolonged wet periods. Rapid increases in water levels in response to heavy short-term rain events decay to background levels within a period of about 10 days. The observed response of the wells to variations in the rainfall and sea level suggests a complicated mix of diffuse and open pathways through a heterogeneous limestone medium.

A close scrutiny of the well response to the forcing of TIDE and RAIN may help to better understand the volumes and rates at which rainwater is captured in storage by the NGLA, and how it travels through the limestone matrix. The mix of time lags at which the wells respond to the RAIN suggest that both the diffuse and open pathways are working to move water through the NGLA independently, with different pathways having different characteristic distributions and response times. Wells respond to widespread heavy rain events with a sharp spike within one day of an event, then return to pre-event levels after about 10 days. Multi-year surpluses or deficits of rainfall tend to be reflected in the water levels at a nearly 2-year time lag. This 2-year memory of the rain forcing suggests that substantial long-term vadose storage is occurring.

The optimization of vadose parameters in Contractor and Jenson's model (Contractor and Jenson, 2000) achieved only about a 30% error-reduction in the model's prediction of water level, suggesting that temporal and spatial variations in vadose zone characteristics are insufficiently known and/or that other processes affecting the temporal and spatial distribution of recharge have yet to be discovered. They noted three plausible sources of error; 1) unknown spatial variability of the hydraulic conductivity in the aquifer, 2) unknown variations in evapotranspiration, and 3) large errors introduced, especially under wet conditions, by the dependency of infiltration and storage on precipitation rates on Guam. The integrated anomalies of the wells used in this report (A16, A20, and BPM1) (Fig 11), and in others not shown, indicate that *all* of these wells are responding similarly to the same long-term forcing. Moreover, A16 and BPM1, in which freshwater is hydraulically connected with the sea, track this forcing in concert. The major surpluses and deficits of integrated well-level anomalies on A16 and BPM1 appear to lag by nearly 2 years similar surpluses and deficits in the integrated rainfall anomaly (Fig. 12) (at A20, the time lag of the response is approximately 6 months). This would suggest that spatial variations in the hydraulic conductivity of the aquifer may not appreciably alter NGLA response to long term variations in forcing, but this hypothesis can be tested only by examining a representative sample of observation wells across the aquifer. As noted, the karst and associated aquifer properties of the area covered in this study differ in both kind and degree from those in the non-argillaceous units of the aquifer. A future study will examine other wells in the other limestone units of the NGLA to evaluate the similarities and differences in behavior from the observations reported in this study.

www.scantopdf.co.uk

REFERENCES

CDM (Camp, Dresser & McKee, Inc.) 1982: Final Report, Northern Guam Lens Study, Groundwater Management Program, Aquifer Yield Report (Prepared by CDM) in association with Barrett, Harris & Associaties for Guam Environmental Protection Agency.)

Contractor, D.N., and J.W. Jenson, 2000: Simulated effect of vadose infiltration on water levels in the Northern Guam Lens Aquifer. *J. Hydrology,* **229**, 232-254.

Guard, C.P., 2000: Monthly and Seasonal Rainfall Climatologies and Distribution Maps for Guam. Technical Report (in press), Water and Environmental Research Institute of the Western Pacific, University of Guam, Mangilao.

Jocson, J.M.U., Jenson, J.W. and Contractor, D.N., 1999: Numerical Modeling and Field Investigation of Infiltration, Recharge, and Discharge in the Northern Guam Lens Aquifer. Technical Report #88, Water and Environmental Research Institute of the Western Pacific, University of Guam, Mangilao.

Maddox, R.A., 1980: Mesoscale convective complexes. *Bull. Amer. Meteorological Soc.,* **61**, 1374-1387.

Mink J.F., and Vacher, H.L., 1997: Hydrogeology of Northern Guam. In: Vacher, H.L & Quinn, T.M. (eds.), *Geology and Hydrogeology of Carbonate Islands*, Developments in Sedimentology #54, Elsevier, Amsterdam, pp. 743-762.

Mylorie, J.E., and H.L. Vacher, 1999: A conceptual view of island karst. In: Palmer, A.N., Palmer, M.V., and I.D. Sasowsky (eds.), Karst Modeling Symposium, Charlottesville, VA, pp. 48-58.

Tracey Jr., J.I., S.O., Schlanger, J.T. Stark, D.B. Doan, and H.G. May, 1964: General geology of Guam, vol. 403-A. U.S. Geological Survey Professional Paper, U.S. Government Printing Office, Washington D.C.

Trenberth, K.E., 1997: The definition of El Niño. *Bulletin of the American Meteorological Society.* **78**, 2771-2777.

Produced with ScanToPDF

www.scantopdf.co.uk

www.scantopdf.co.uk

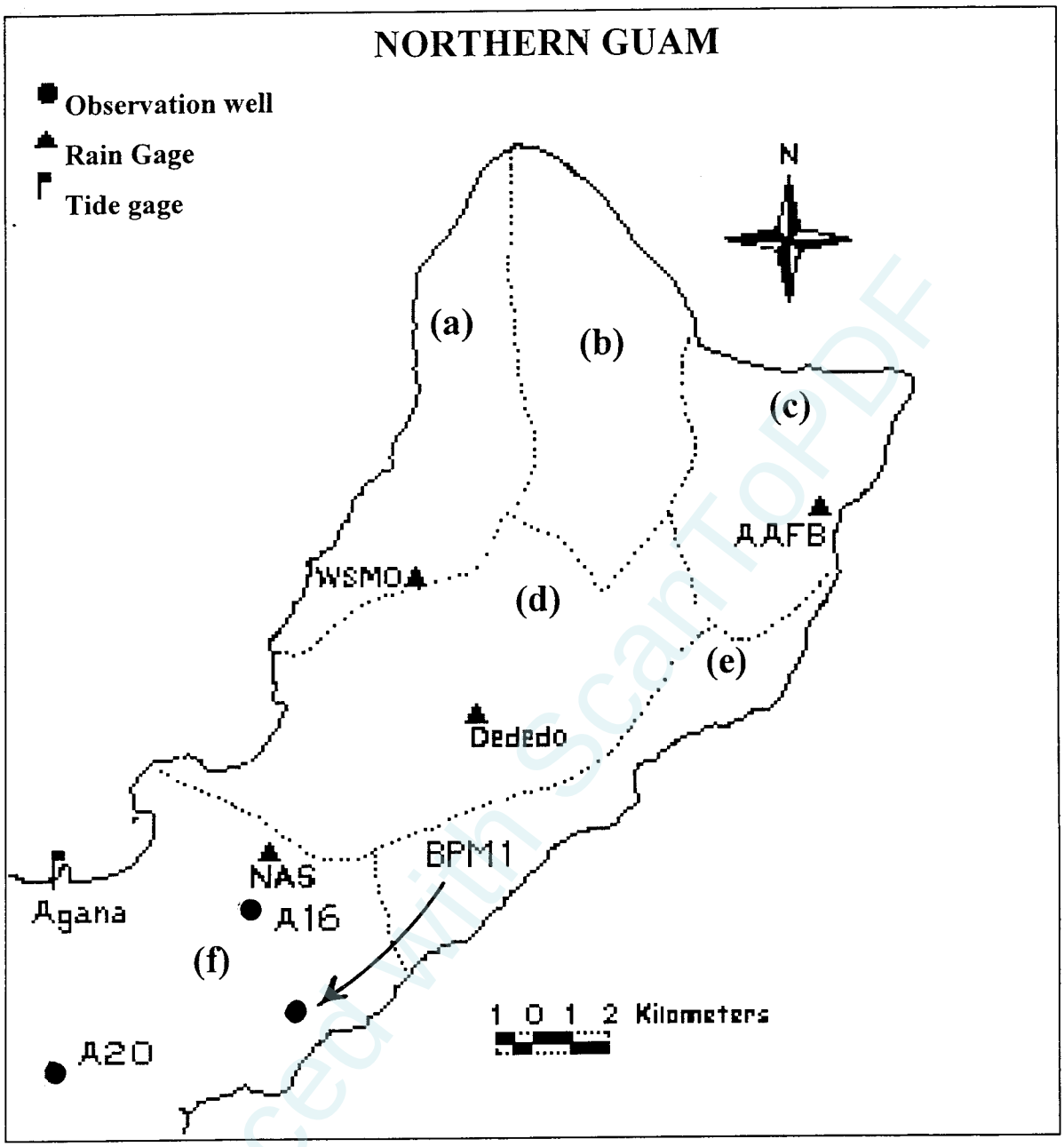

Figure 1. A map of northern Guam showing the locations of cited wells, rain gages, and the Agaña Boat Basin tide gage. The dotted lines indicate the boundaries of the sub-basins of the northern Guam lens aquifer: (a) Finagayan, (b) Agafa Gumas, (c) Andersen, (d) Yigo-Tumon, (e) Mangilao, and (f) Agaña.

Produced with ScanToPDF

www.scantopdf.co.uk

www.scantopdf.co.uk

(a)

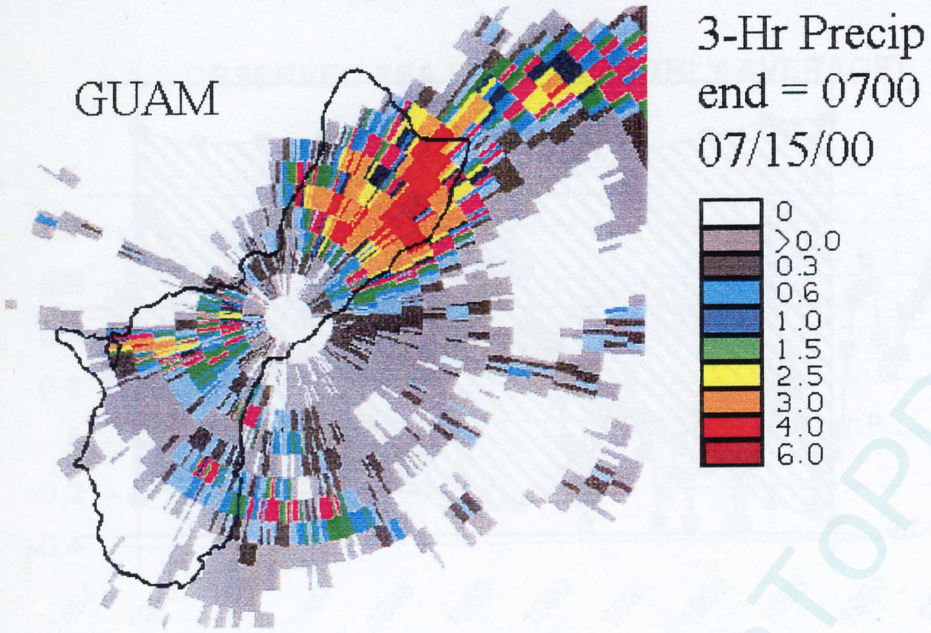

(b)

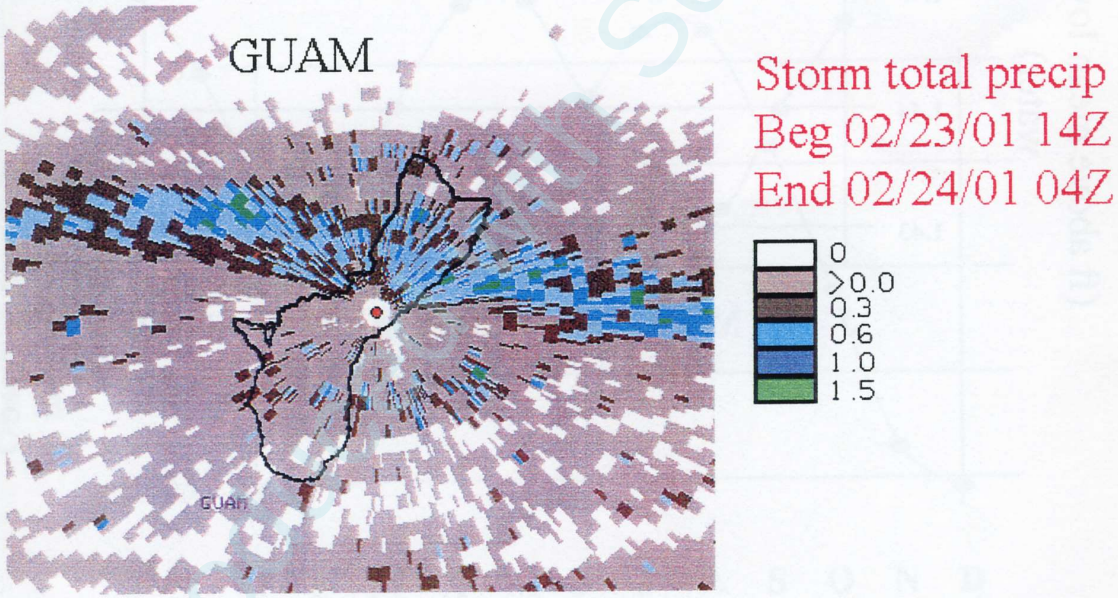

Figure 2. (a) Three-hour integrated rainfall during an isolated thunderstorm event (July 15, 2000). Maximum rainfall values exceeded 6 inches in a small area of northern Guam. (b) The storm-total precipitation algorithm depiction of a narrow swath of nearly one inch of rain that was deposited by a band of tradewind showers during Guam's dry season. Both panels are examples of NEXRAD integrated rainfall products.

www.scantopdf.co.uk

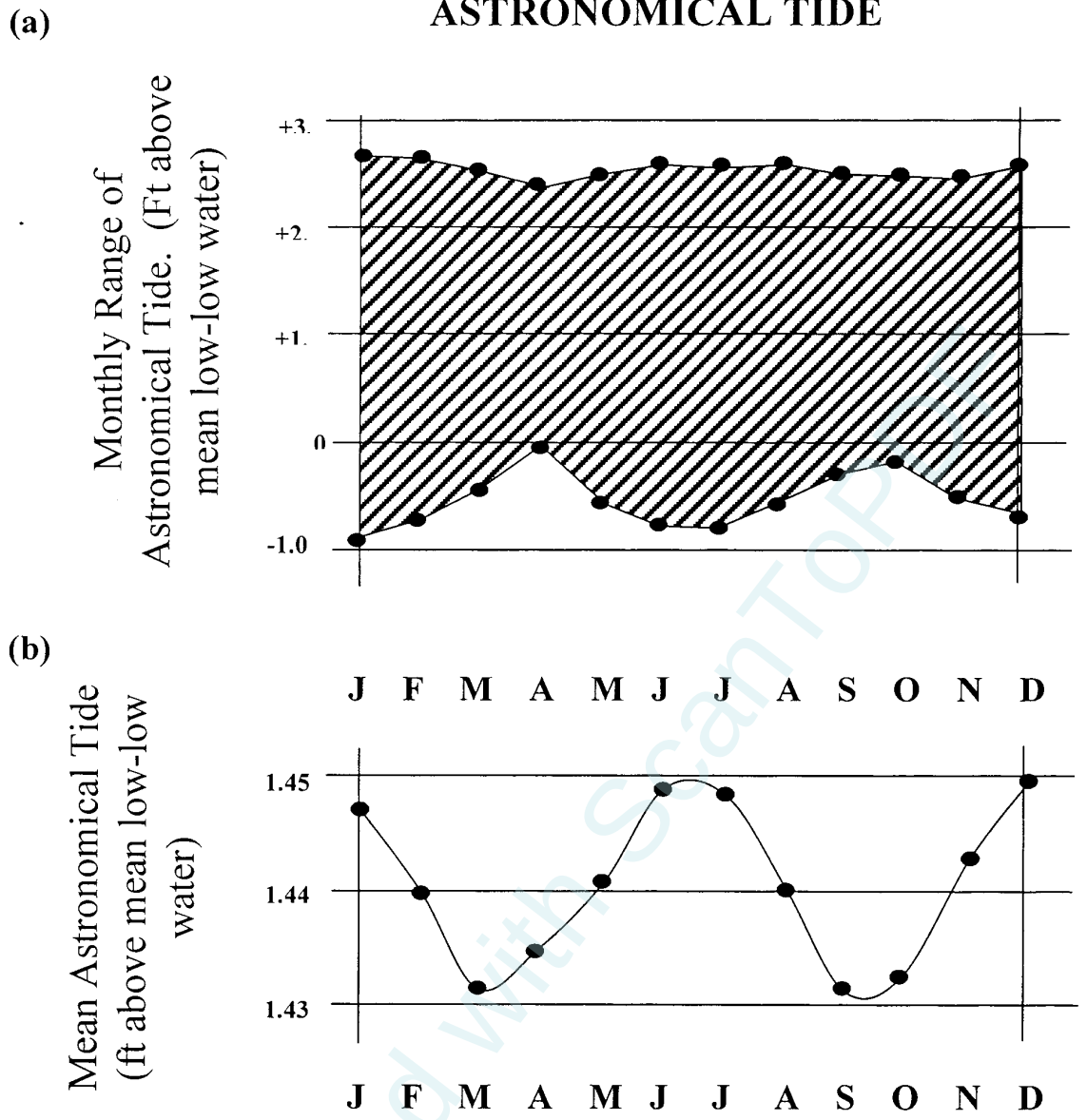

Figure 3. Annual variations of the astronomical tide: (a) the monthly range, and (b) the monthly mean height.

Produced with ScanTOPDF

www.scantopdf.co.uk

www.scantopdf.co.uk

(a)

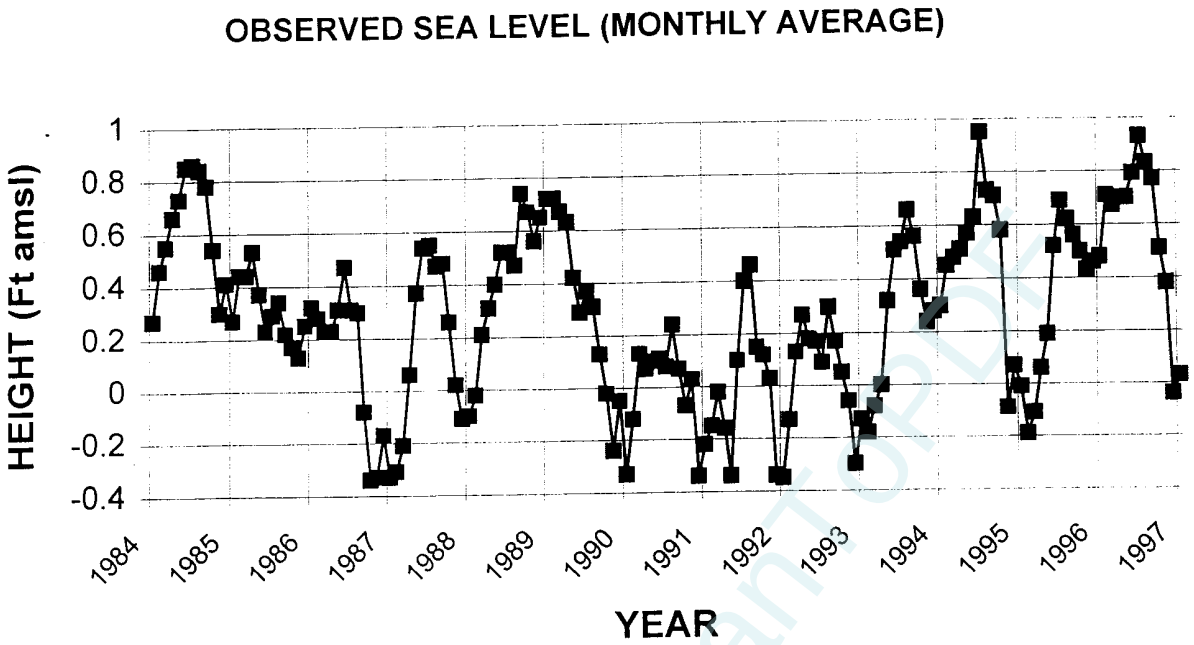

(b)

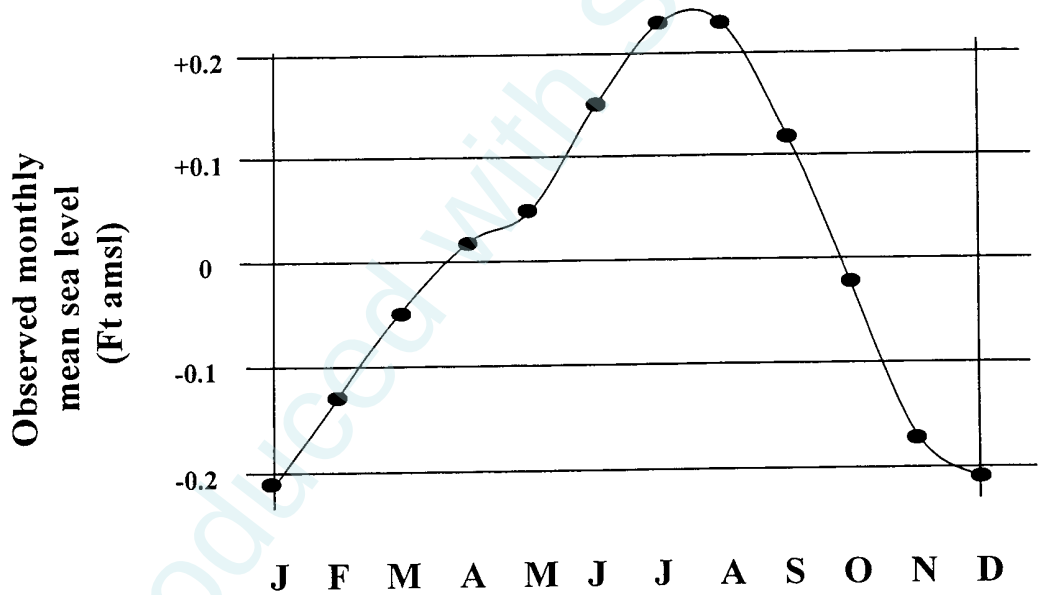

Figure 4. Observed sea level: (a) monthly averages, and (b) annual cycle.

Produced with ScanTopPDF
www.scantopdf.co.uk

www.scantopdf.co.uk

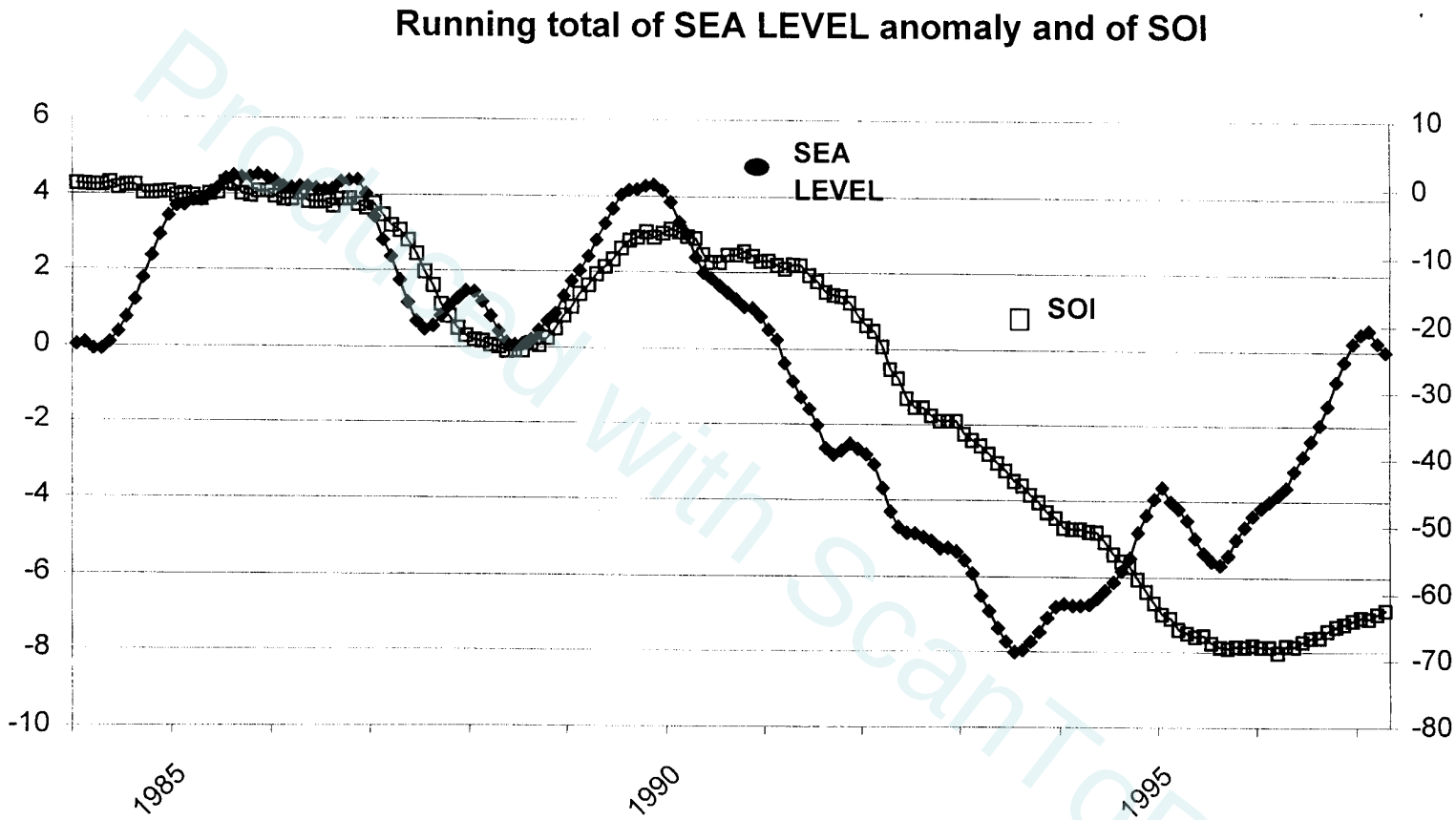

Figure 5. Integrated anomalies of the Guam monthly SEA LEVEL and of the Southern Oscillation Index (SOI). The similar profiles of the curves suggest that the Guam SEA LEVEL is related to the SOI in such a way that when the SOI is lower than normal, the seal level is lower than normal. This is physically consistent with the fact that the SOI is strongly correlated with the anomaly of the surface wind in the tropical Pacific basin: high SOI, strong easterlies; low SOI, weaker easterlies.

Produced with scanTOPDF
www.scantopdf.co.uk
www.scantopdf.co.uk

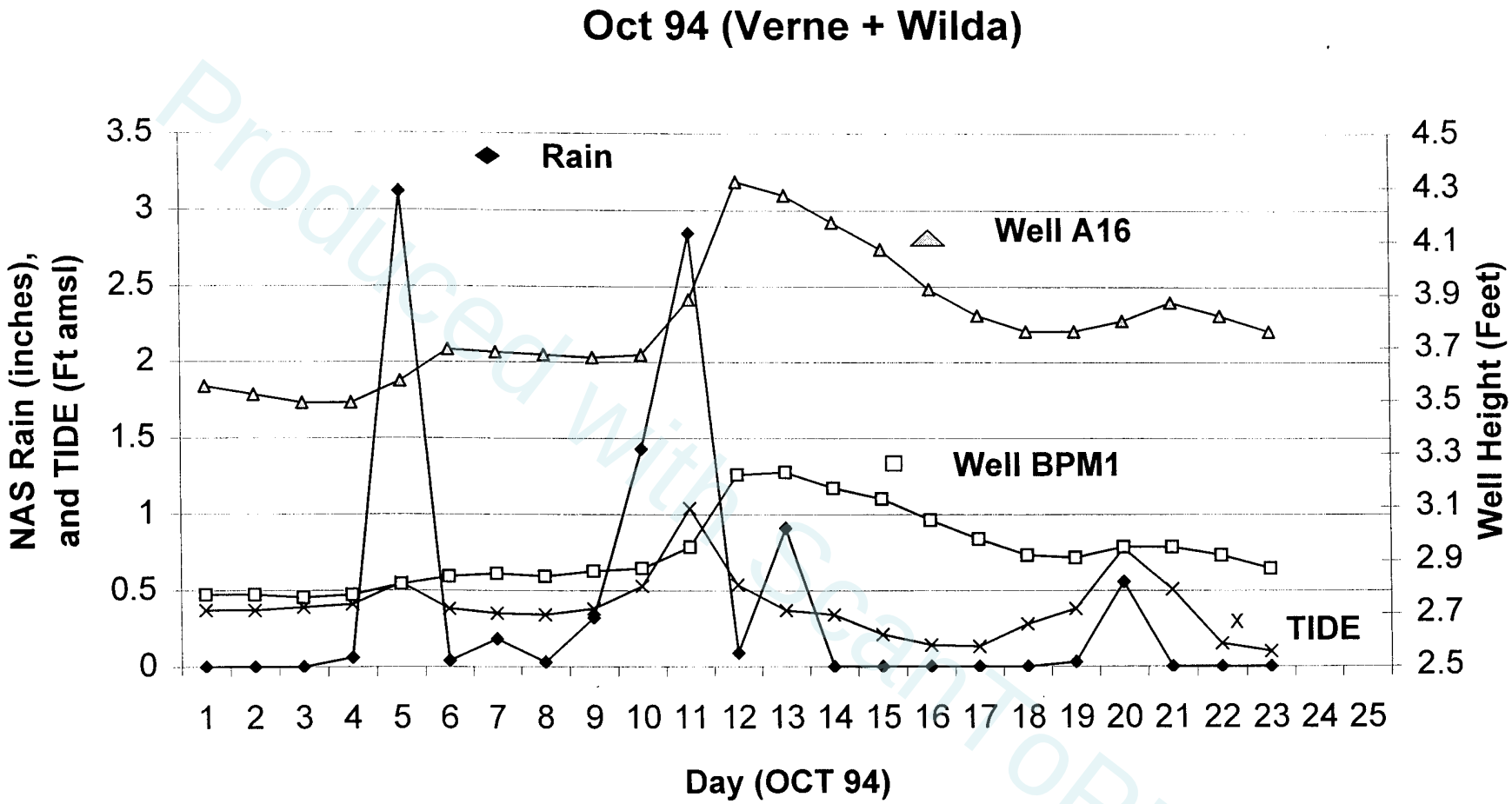

Figure 6. A time series of the wind, rain and well levels at BPM1 and A16 during October 1994 reveals some of the complicating factors affecting the relationships among the several time series. For example, the apparent correlation of TIDE and RAIN is an artifact of wave set up during the near passage of tropical cyclones.

Produced with ScantoPDF
www.scantopdf.co.uk
www.scantopdf.co.uk

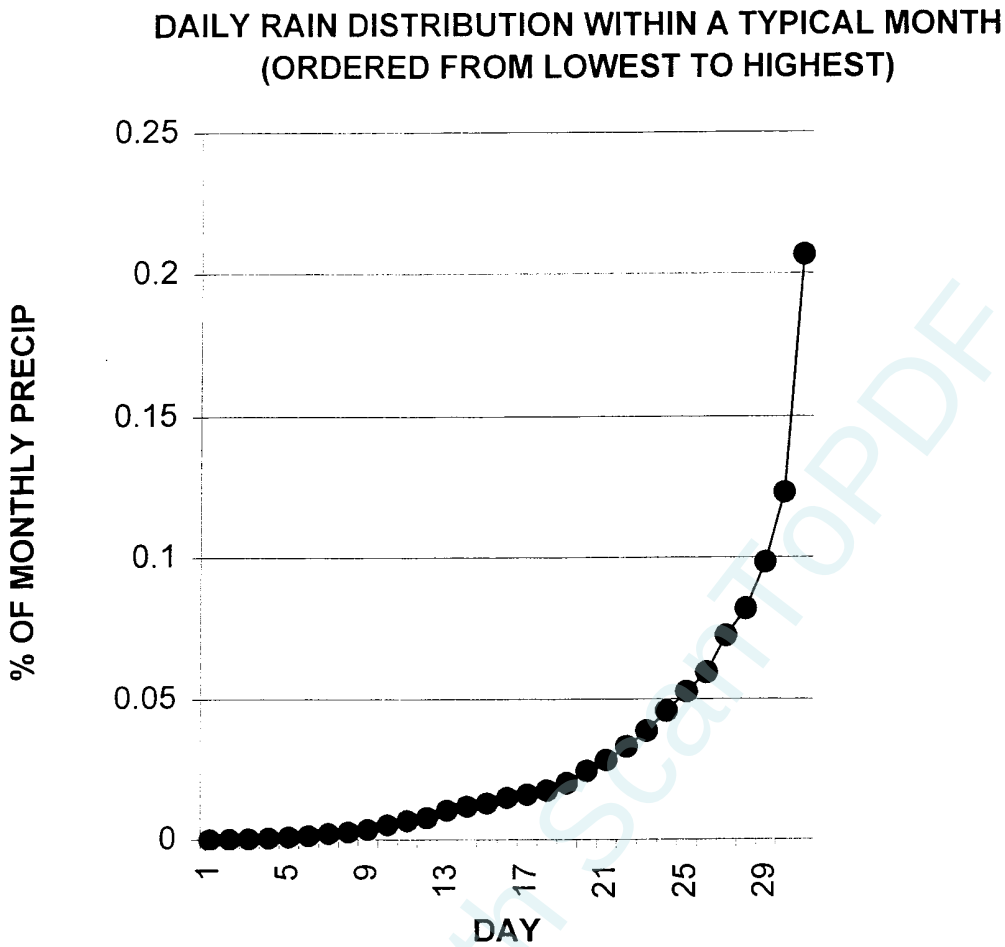

Figure 7. The typical distribution of daily rainfall totals within a month expressed as a percent of the monthly total, and ordered from lowest to highest. This curve is the average of six August's and six July's.

Produced with ScanToPDF

www.scantopdf.co.uk

www.scantopdf.co.uk

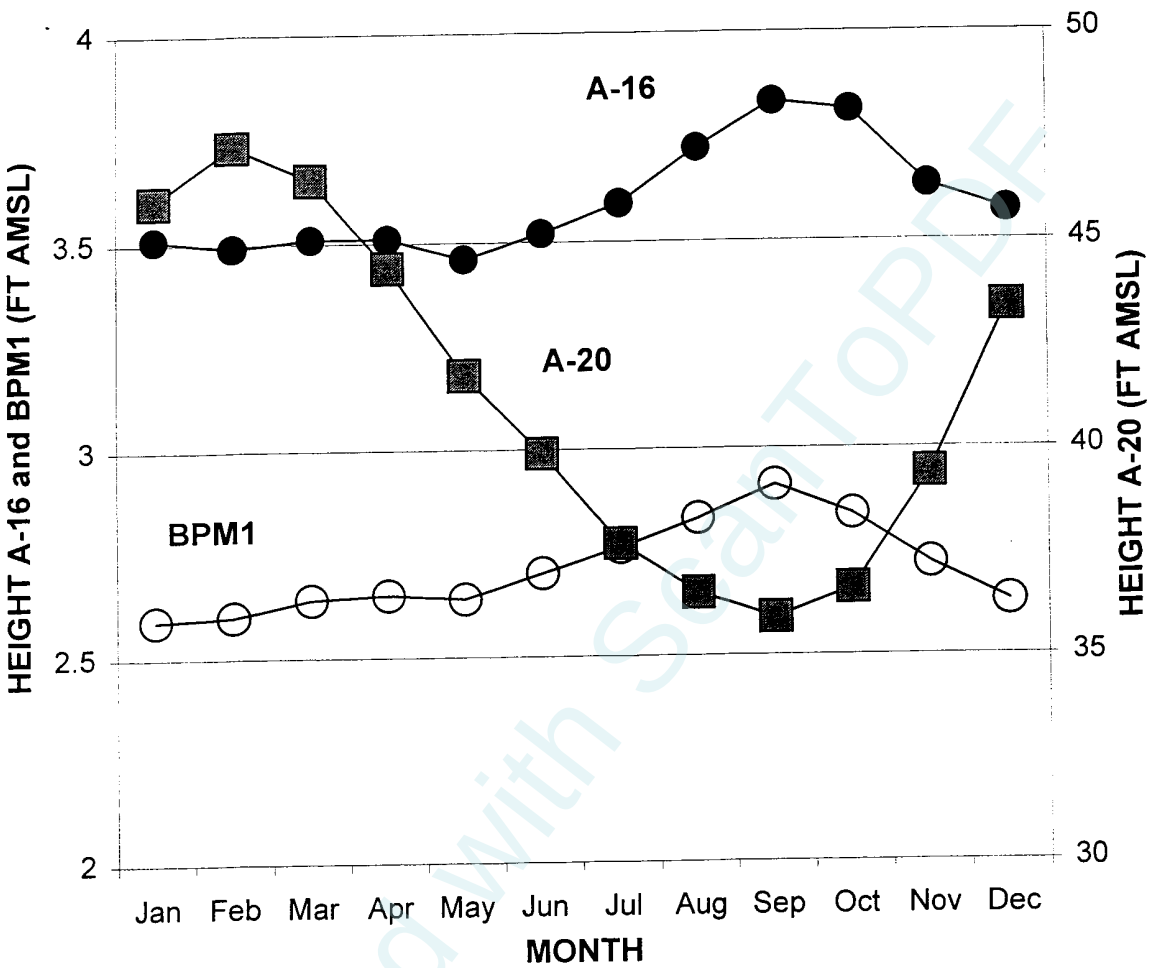

Figure 8. Mean monthly well levels at BPM1, A16, and A20.

Produced with ScanTOPDF
www.scantopdf.co.uk

www.scantopdf.co.uk

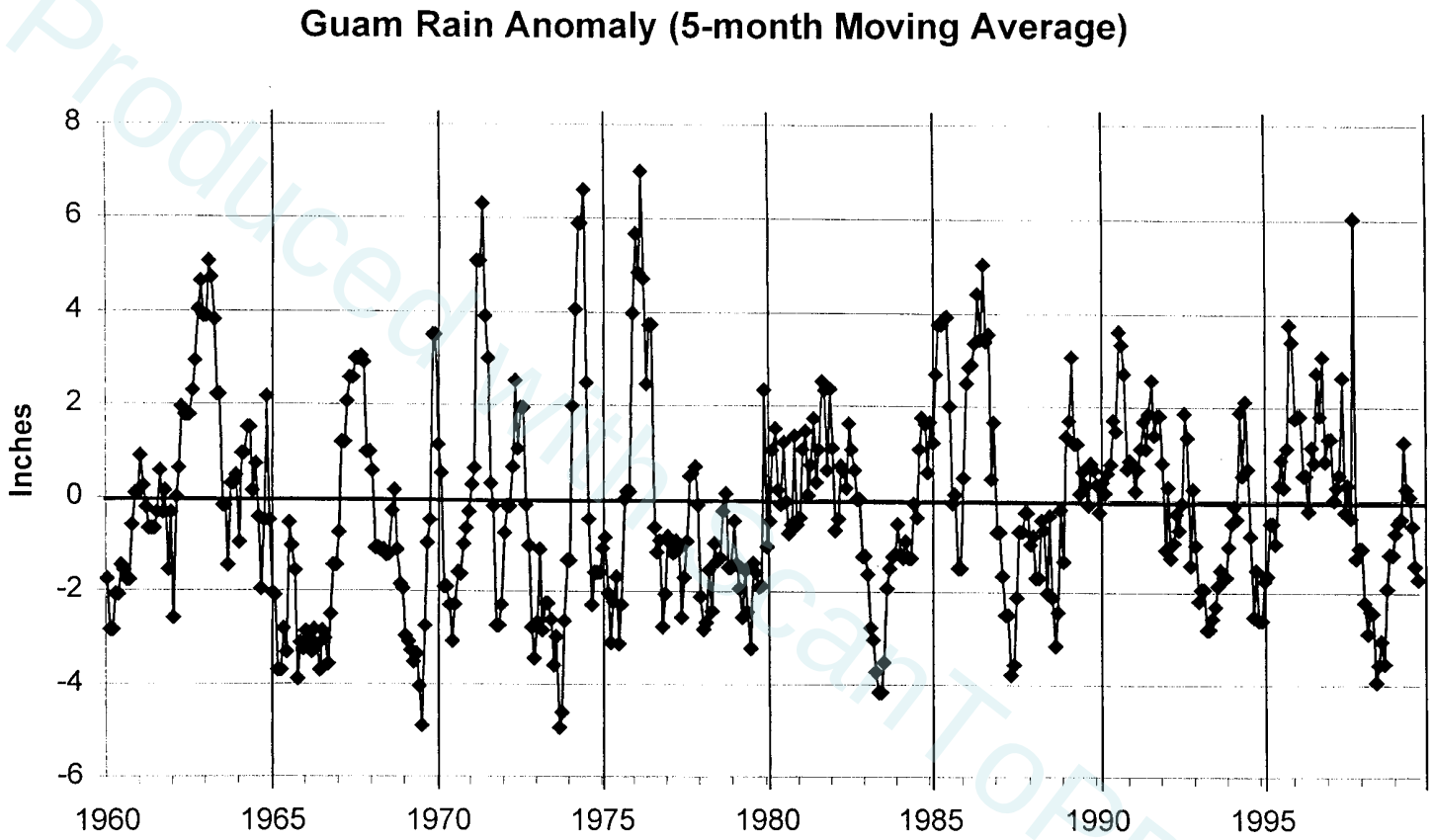

Figure 9. A five-month moving average of Guam's (NAS) monthly rainfall anomaly.

Produced with ScanToPDF
www.scantopdf.co.uk
www.scantopdf.co.uk

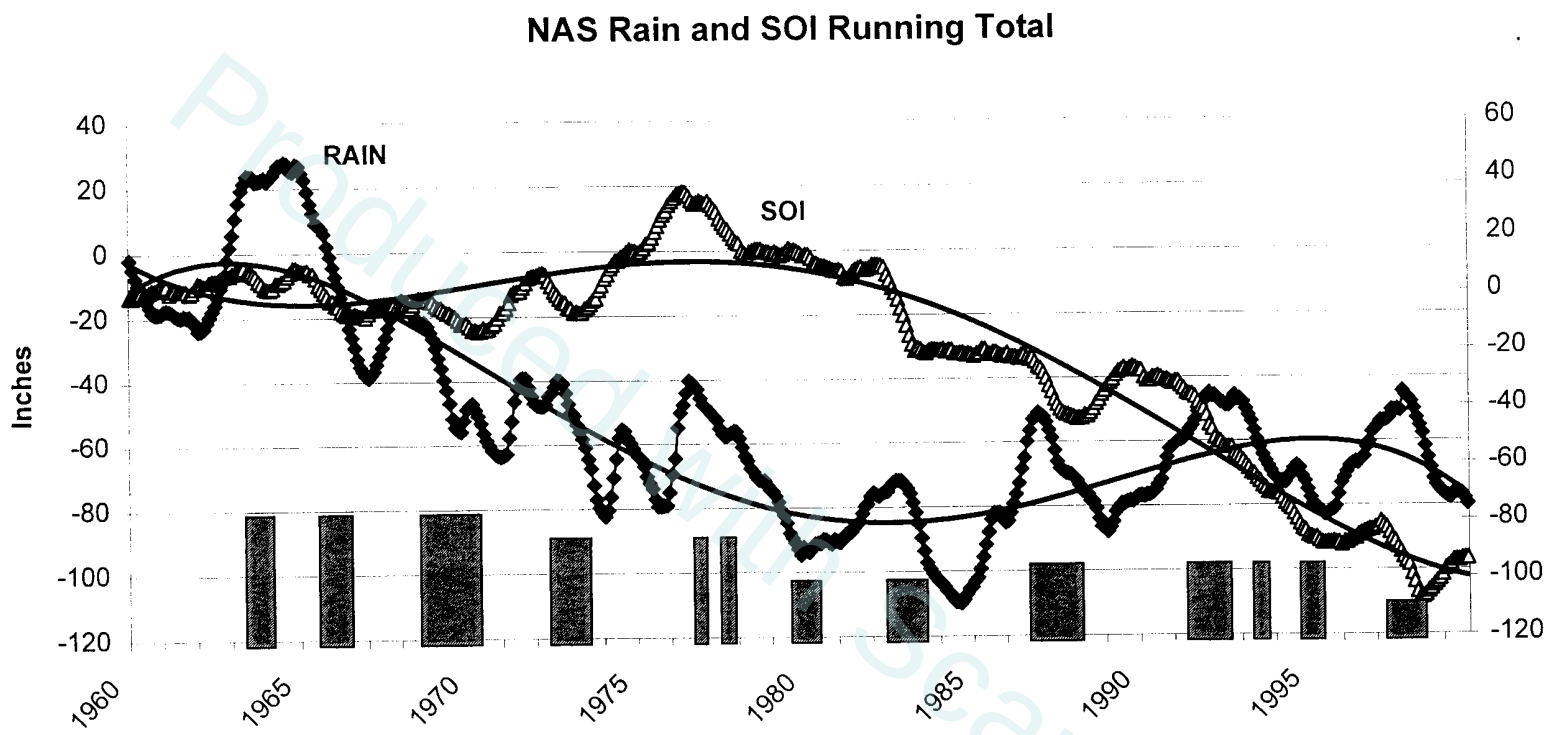

Figure 10. Running accumulations of the rainfall anomaly at NAS and of the raw values of the Southern Oscillation Index (SOI). Shaded boxes are El Niño periods as defined by Trenberth (1997). Box height has no other meaning than to avoid overlap with data. Solid lines are the best-fit 4th order polynomial.

Produced with ScanToPDF
www.scantopdf.co.uk
www.scantopdf.co.uk

(a)

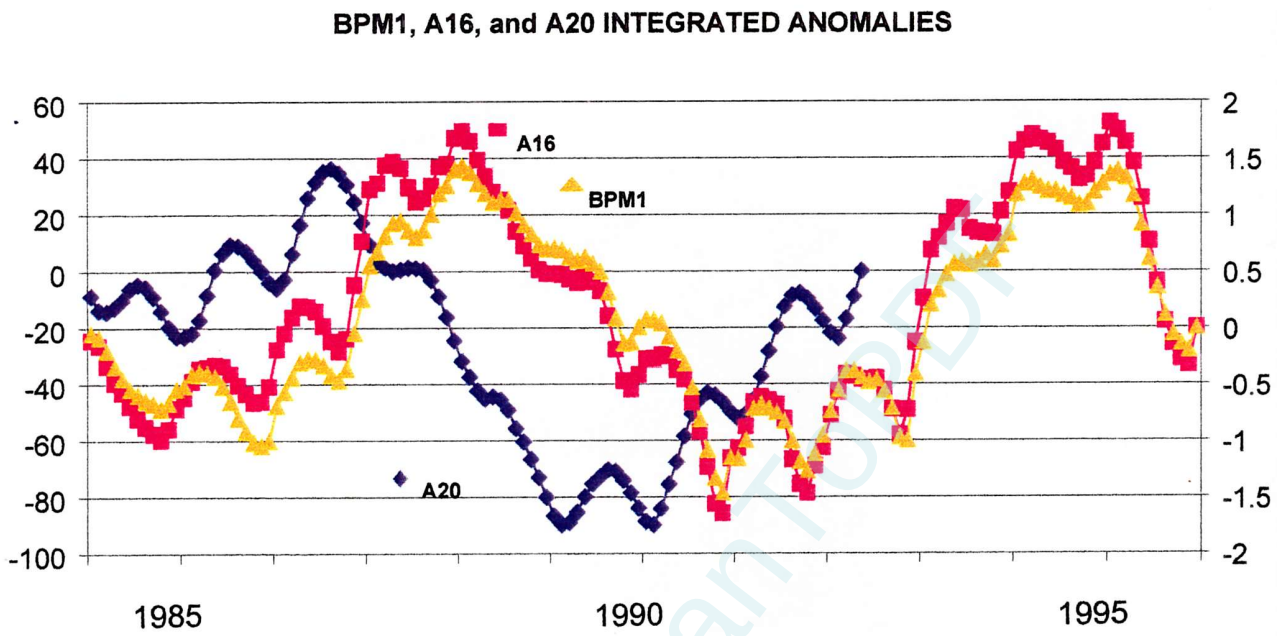

(b)

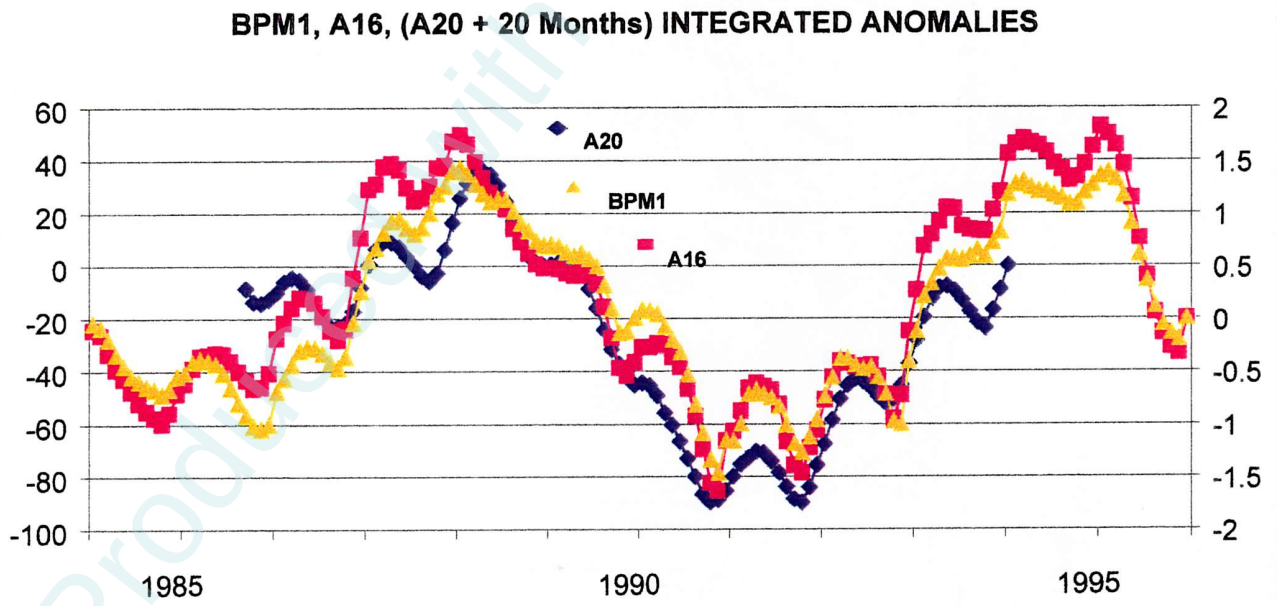

Figure 11. (a) Integrated anomalies of the well level at A16, A20, and BPM1. Multi-year deficits and surpluses are clearly evident. (b) The nearly 2-year offset of A20 with respect to the other two wells indicates that these wells are responding to the long-term rain signal at different time lags. Work on this topic is ongoing, and will be discussed in a future technical report.

Produced with ScanToPDF
www.scantopdf.co.uk
www.scantopdf.co.uk

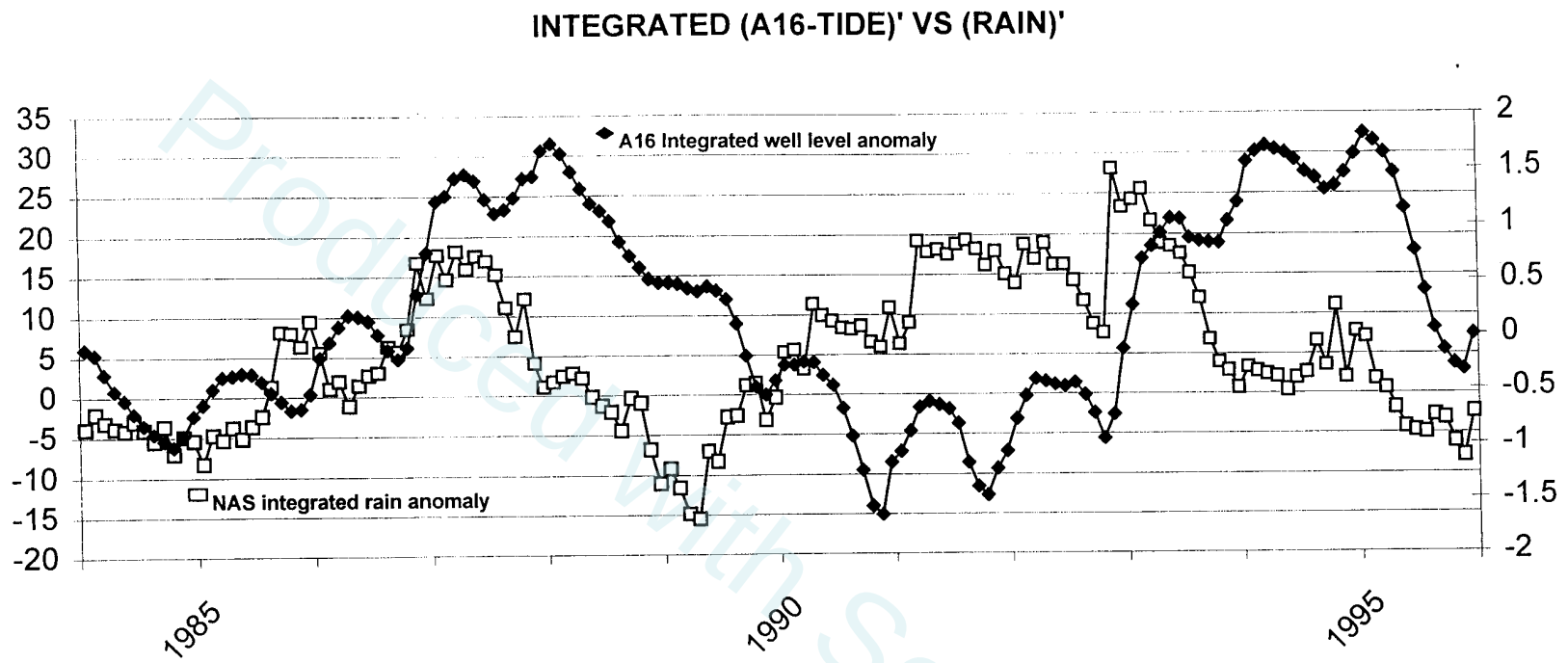

Figure 12. Integrated anomalies of the A16 well level (de-Tided), and of the monthly rainfall anomaly at NAS. There appears to be a lag of approximately 2 years between the major multi-year peaks and dips of the well level with those in the RAIN time series. (The Annual cycle has been removed from the RAIN, but not from A16.)

Produced with ScanToPDF
www.scantopdf.co.uk
www.scantopdf.co.uk

(a)

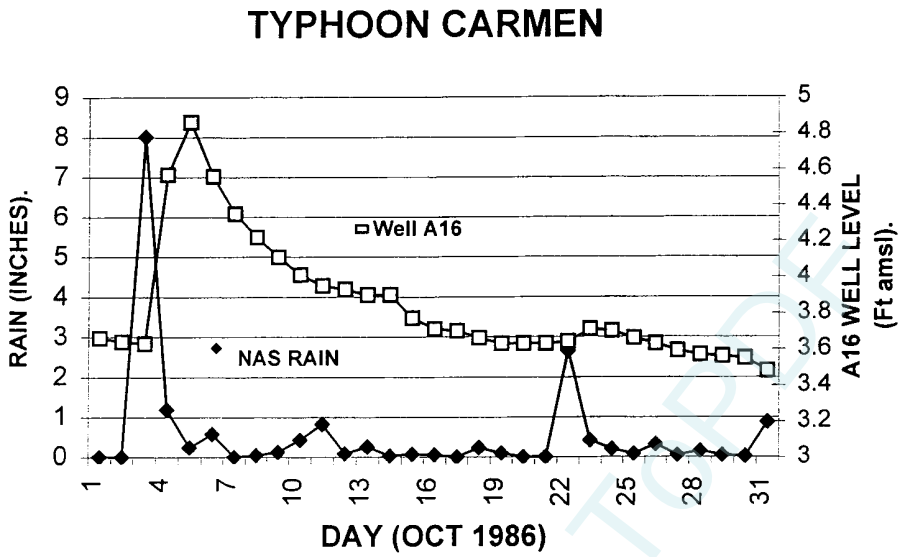

(b)

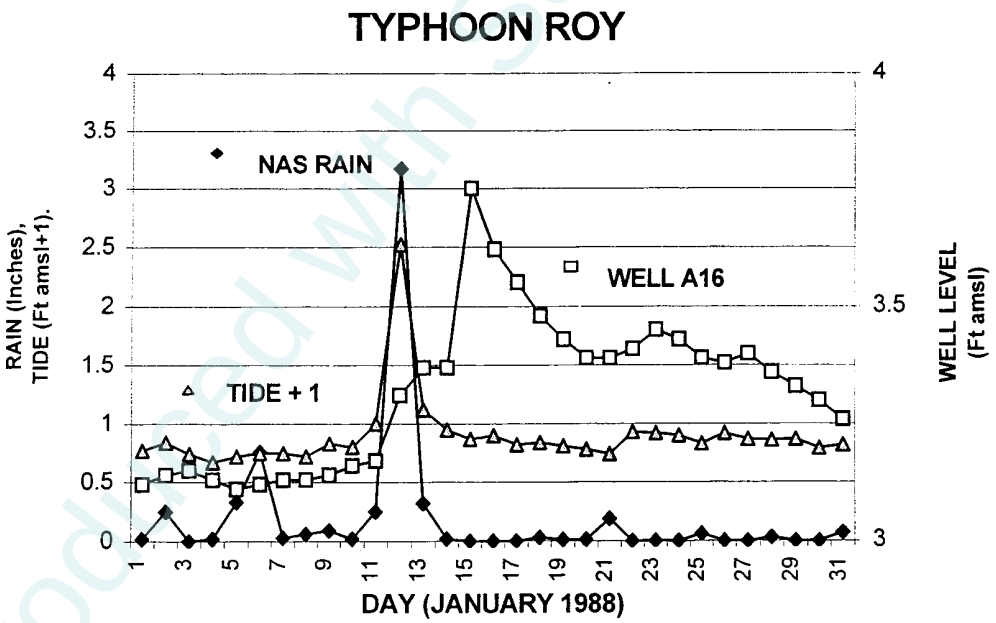

Figure 13. Response of the water level in Well A16 to island-wide extreme rain events during typhoons: (a) Typhoon Carmen; and (b) Typhoon Roy. The Daily average TIDE has been included in (b) to show the response of TIDE at the Agaña Boat Basin to strong northwest wind.

Produced with Scan TOPDF
www.scantopdf.co.uk

www.scantopdf.co.uk

(a)

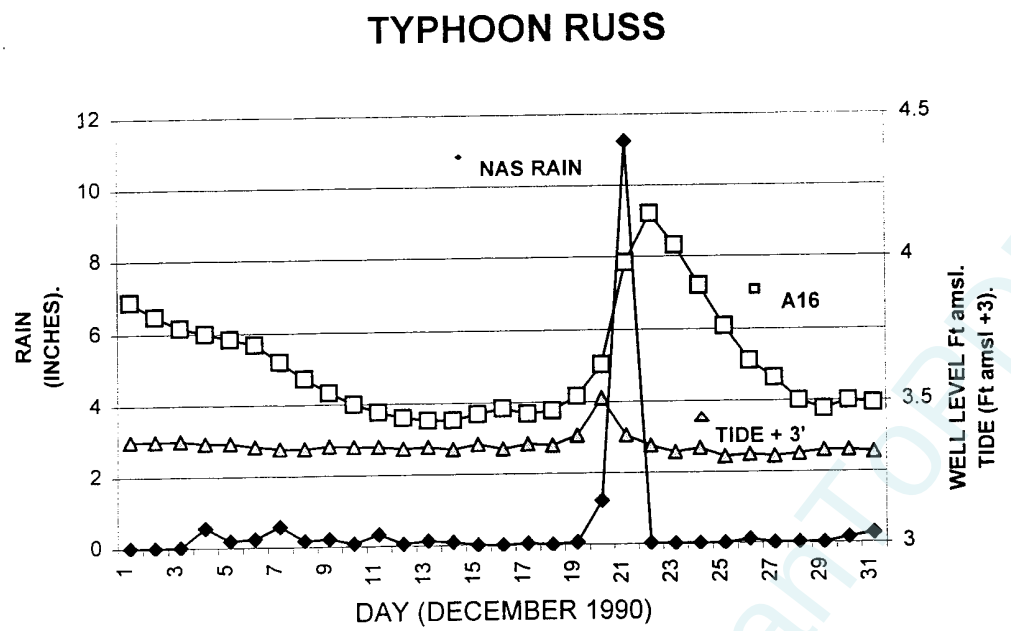

(b)

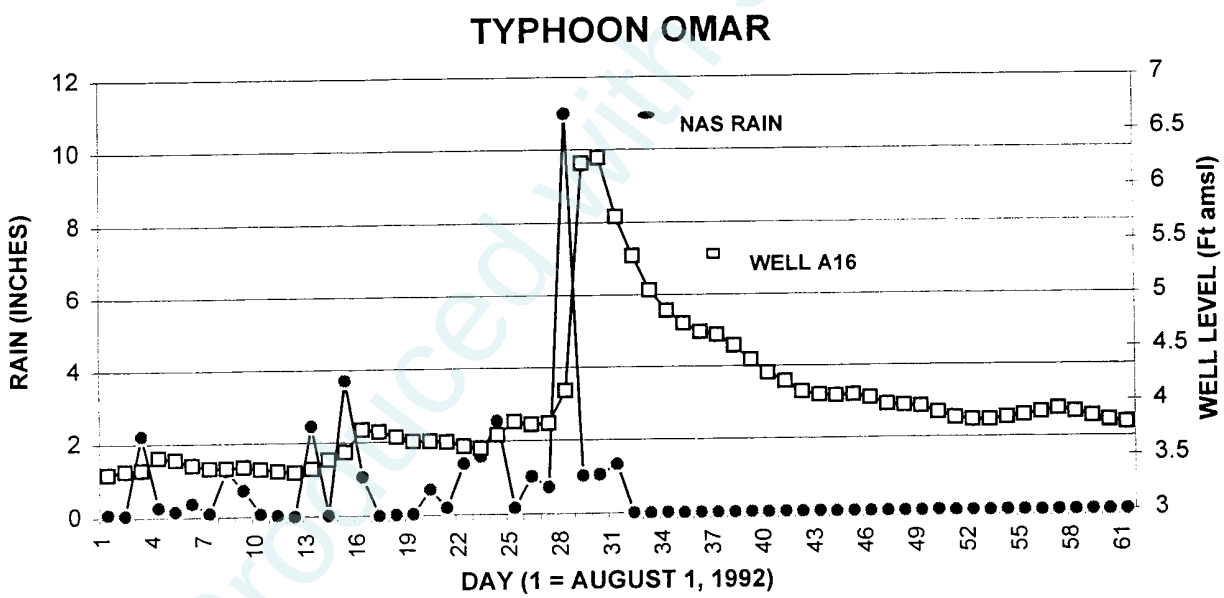

Figure 14. Response of the water level in Well A16 to island-wide extreme rain events during typhoons: (a) Typhoon Russ; and (b) Typhoon Omar. The daily average TIDE has been included in (a) to show the response of the TIDE at the Agaña Boat Basin to strong northerly winds in advance of RUSS.

Produced with ScanTOPDF
www.scantopdf.co.uk
www.scantopdf.co.uk

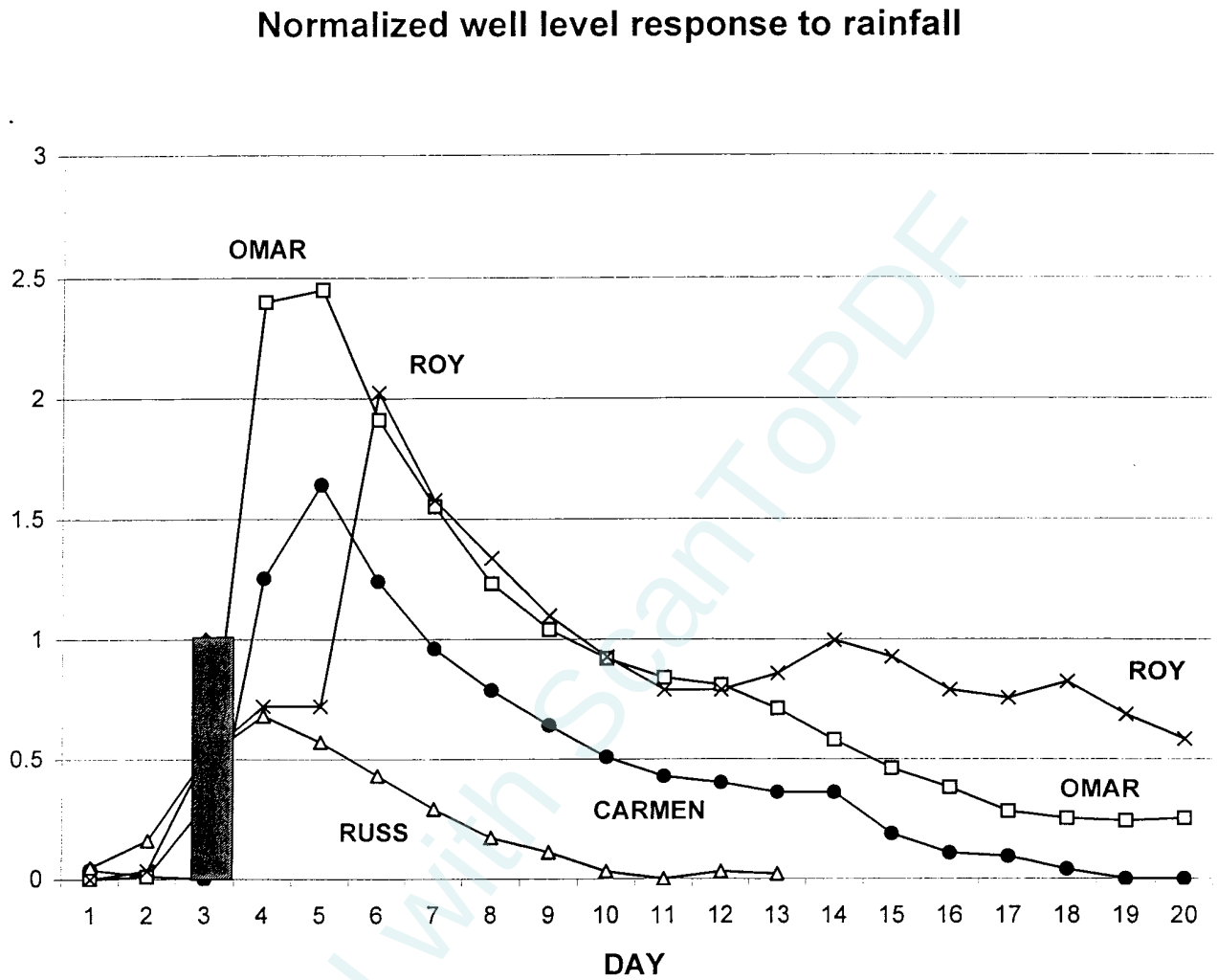

Figure 15. Well A16 response to heavy rain events produced by the indicated typhoons. The well response has been normalized to the peak 24-hour rain amount (solid bar).

Produced with ScanTOPDF

www.scantopdf.co.uk

www.scantopdf.co.uk

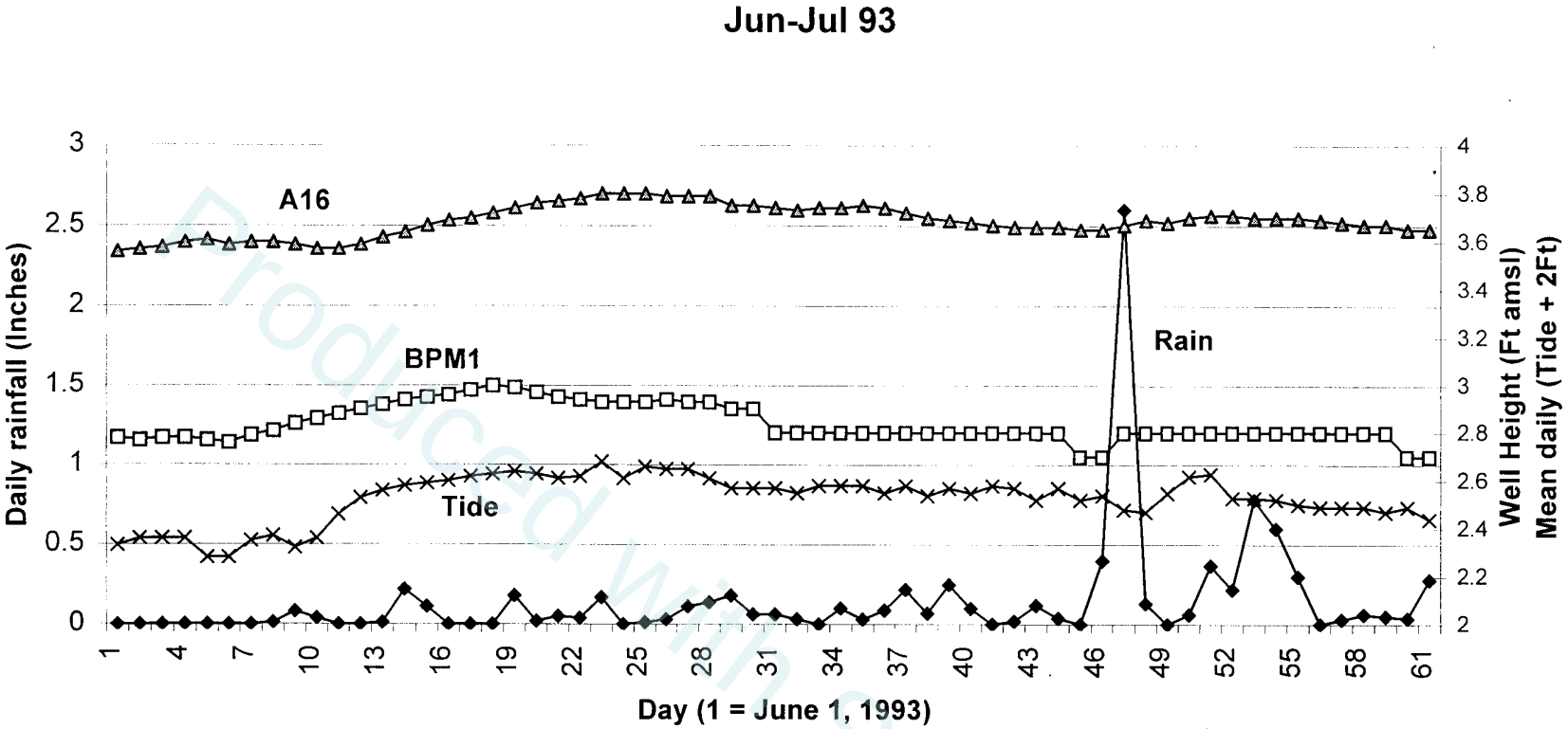

Figure 16. The first heavy daily rain event following the prolonged dry spring of 1993 has little effect on the level of wells A16 and BPM1. The daily mean sea level appears to dominate changes in well level.

Produced with scantoPDF
www.scantopdf.co.uk
www.scantopdf.co.uk

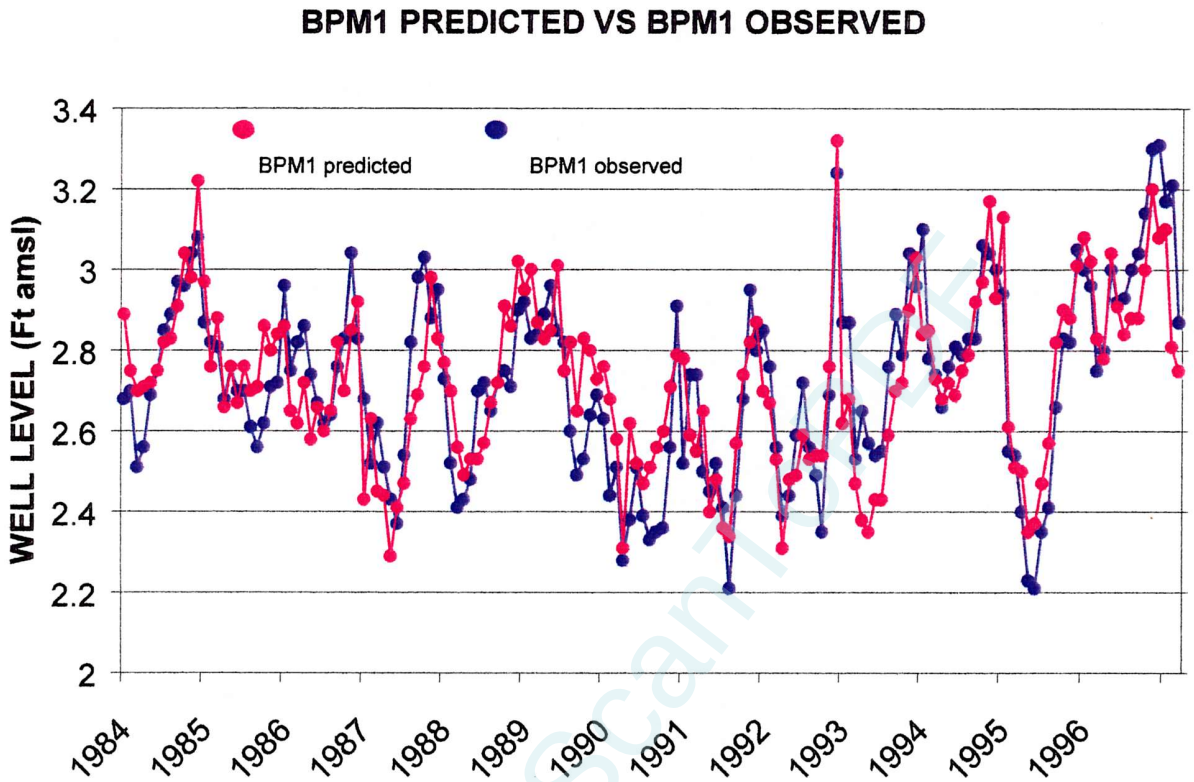

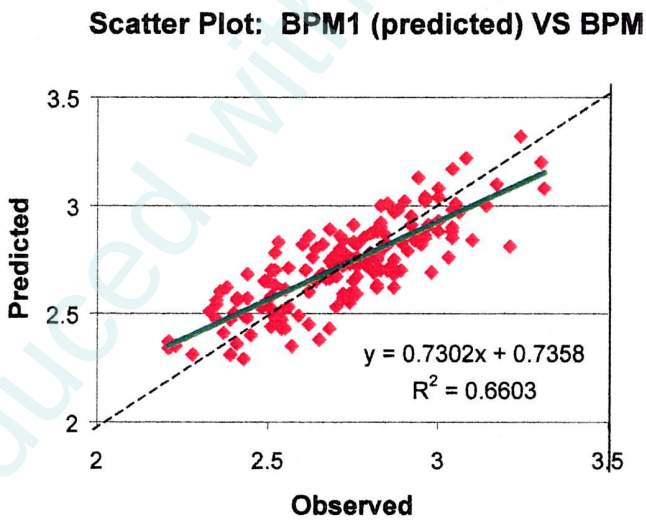

Figure 17. The predicted level of well BPM1 from RAIN and TIDE versus the observed level (top). Scatter plot of the residuals (bottom) shows that a bias is present: the predictions of the highest well levels tend to be too low, and the predictions of the lowest well levels tend to be too high. Green line is the least-squares best-fit, and the dashed line indicates where the predicted value equals the observed.

Produced with ScanToPDF
www.scantopdf.co.uk
www.scantopdf.co.uk

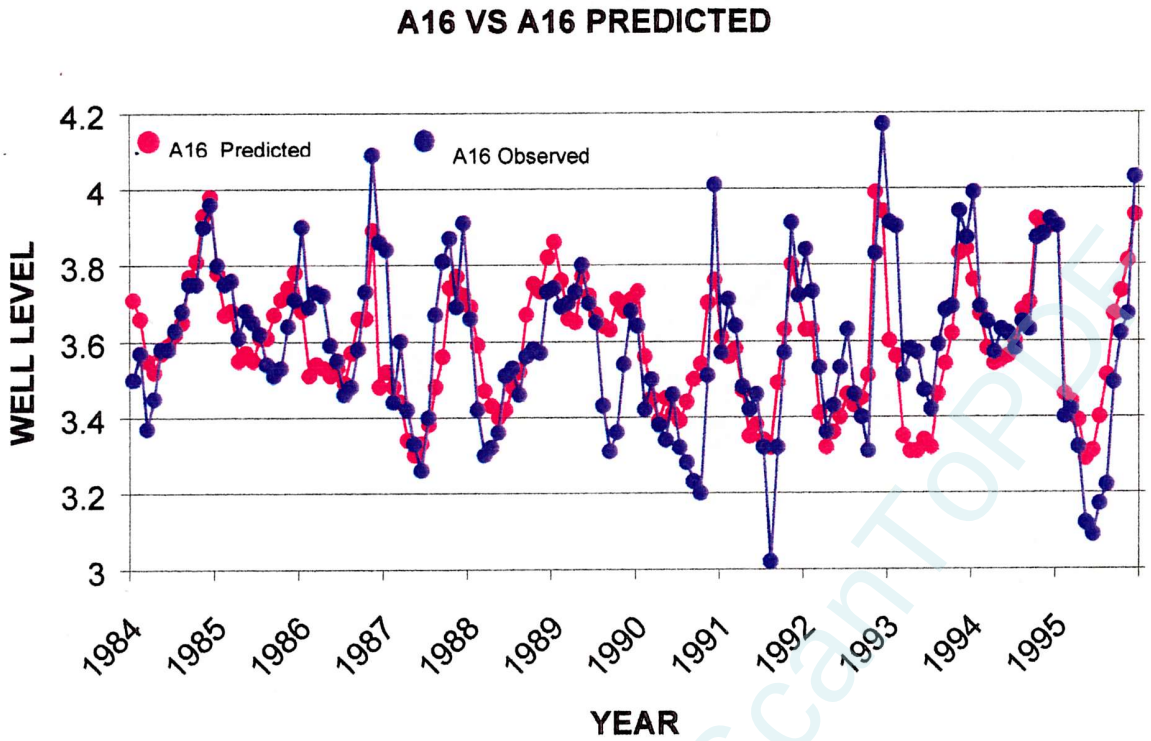

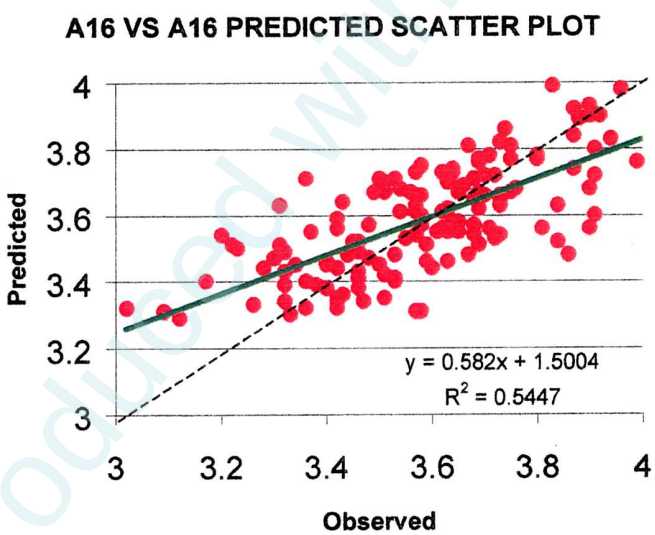

Figure 18. The predicted level of well A16 from RAIN and TIDE versus the observed level (top). Scatter plot of the residuals (bottom) shows that a bias is present: the predictions of the highest well levels tend to be too low, and the predictions of the lowest well levels tend to be too high. Green line is least squares best-fit, and the dashed line indicates where the predicted equals the observed.

Produced with ScanTOPDF
www.scantopdf.co.uk
www.scantopdf.co.uk

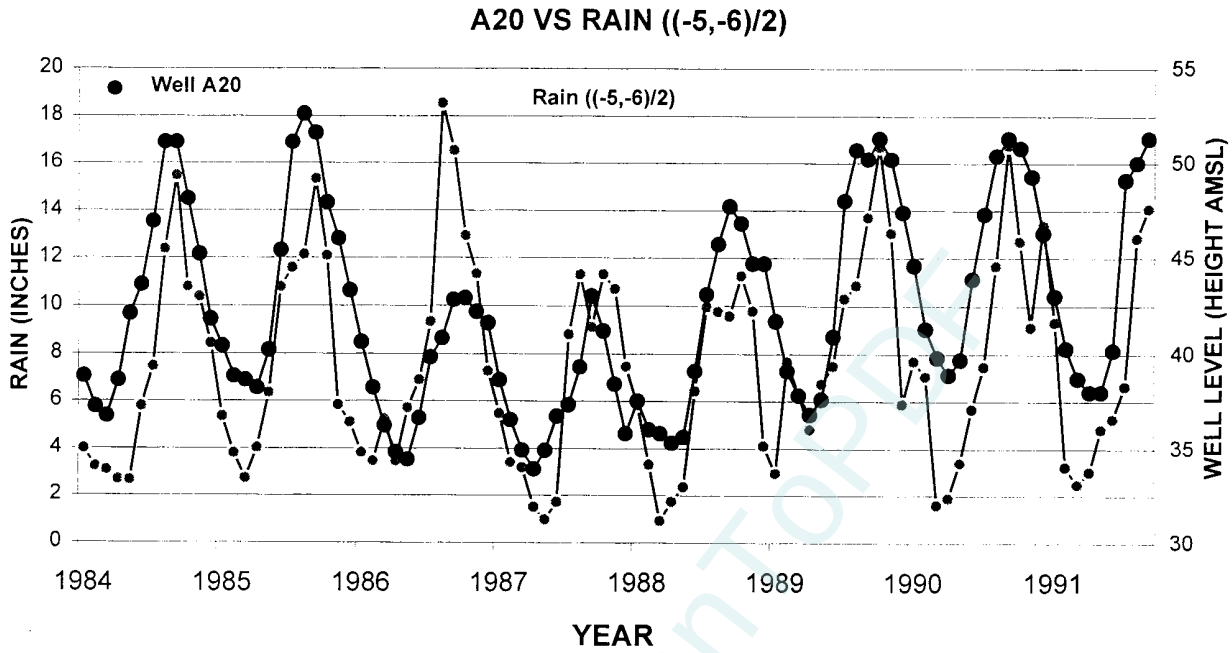

Figure 19. Well A20 monthly water levels superimposed over the monthly values of a derived RAIN variable: one-half the rain at lag 6 months plus one-half the rain at lag 5 months. The cross-correlation coefficient of this RAIN variable with the well level at A20 is +.73.

Produced with ScanTopPDF

www.scantopdf.co.uk